SHIMADZU
Excellence in Science

NEWS 01 2015

From a "local workshop" to a global player

2015, Shimadzu celebrates its 140th anniversary: a success story

The secrets of a Swiss watch

»In our lab we R.E.A.C.H. the very secrets of matter«

Hidden danger

LCMS-8050 – Faster and more sensitive detection of mycotoxins in baby food

CONTENT

APPLICATION

»It is the dose that makes the poison« New ICPE-9800 series 4

Animal kingdom suffering from plastic wastes 6

The secrets of a Swiss watch – »In our lab we R.E.A.C.H. the very secrets of matter« 12

Testing wine bottles – Non-destructive quality control 16

Coffee inspired not only science – Particle measurement using the SALD-2300 18

Hidden danger – Faster and more sensitive detection of mycotoxins in baby food 20

Biomass fuel: can algae make the wheels go round? – Monitoring of algae growth 22

Universal testing machine qualifies electronic components 28

High sensitivity meets robustness 30

PRODUCTS

Small yet high-performance – New UV-VIS spectrophotometer UV-1280 8

New milestone in ICP-OES technology 9

Insights on molecular level – iMScope *TRIO* 10

Sweet secrets analyzed fast and easily 24

More freedom of choice – New features in TOC-Control L-software 26

Performance meets design 31

Extended analysis possibilities – Special accessories for the UV-3600 Plus 32

LATEST NEWS

From a "local workshop" to a global player 2

Selenium in blood serum – Atomic absorption spectroscopy for trace analysis 14

Shimadzu employees are socially engaged 27

NEWS – Shimadzu's customer magazine is also available as WebApp (for iOS and Android) via: www.shimadzu-webapp.eu or as app for iPhone in the AppStore.

From a "local workshop" to a global player

Shimadzu celebrates its 140th anniversary

He was the son of a craftsman of Buddhist altars, but driven to manufacture instruments for physics and chemistry. He attended the Physics and Chemistry Research Institute, where he gained experience with a variety of technologies and fields of expertise. He was convinced that Japan as a country with few natural resources should work towards becoming a leader in science. At the door-step from the industrial revolution to the scientific age, he founded in 1875 his own business in Kiyamachi, Kyoto. His name was Genzo Shimadzu.

In 1877, he succeeded in launching the first manned balloon flight in Japan. One year after exploration of X-rays through Conrad Röntgen in Germany, Genzo Shimadzu took the first X-ray images in Japan. In the following years, he created the first commercial X-ray system in Japan and started the production of machines for materials development. In 1930, the emperor awarded Genzo Shimadzu one of the Top 10 inventors in the history of the country.

140 years later and celebrating its anniversary in 2015, Shimadzu is one of the worldwide leading manufacturers of analytical instrumentation and diagnostic imaging systems. Its technologies are used as essential tools for quality control of consumer goods and articles of daily use, in health care as well as in all areas of environmental and consumer protection. Spectroscopy, chromatography, environmental

analysis, balances, biotechnology, material testing and medical technology make up a homogeneous yet versatile offering. Along with many "industry first" technologies and products Shimadzu has created and invented since 1875, there has also been the exceptional awarding of the 2002 Nobel Prize for Chemistry to Shimadzu engineer Koichi Tanaka for his outstanding contributions in the field of mass spectrometry.

As a global player, Shimadzu operates production facilities and distribution centers in 76 countries, with more than 10,000 employees worldwide. For over 45 years the European headquarters has been located in Europe.

Shimadzu's analyzers and equipment are applied in the chemical, petrochemical and pharmaceutical industry, life sciences and biotech, cosmetics, semiconductor and nutrition industry as well as in the flavors and fragrances business. Research institutes, privately run laboratories, administrations and universities complete the list of clients. The systems are used in routine and high-end applications, process and quality control as well as R&D.

"Excellence in Science"

Since 2012, Shimadzu's brand value proposition is expressed through the new claim "Excellence in Science" representing Shimadzu's scientific and technological approach to always provide business and research solutions with the most modern analytical and diagnostic systems ensuring better product, consumer, and patient safety. Numerous world firsts which have become industrial standards today as well as increasingly sensitive measuring methods substantiate this claim.

Shimadzu's new "Laboratory World" in Duisburg, Germany is an example how to fulfill this brand promise. On over 1,500 m^2, most-modern testing and training facilities were created for Shimadzu's entire product range – from chromatographs, spectrophotometers, TOC analyzers, mass spectrometers and material testing machines.

A few selected milestones:

- In **1896**, only one year after Dr. Roentgen discovered X-rays, Shimadzu succeeded in producing an X-ray image
- In **1909**, Shimadzu developed the first medical X-ray device made in Japan. Ever since then, Shimadzu has remained a pioneer in the field of medical X-ray devices
- **1934**: with the development of Japan's first spectrograph, Shimadzu advanced into the field of analytical instruments
- **1936**: Begin to manufacture aircraft equipment
- In **1951**, Shimadzu began to increase the number of exports to global markets
- **1956**: Development of Japan's first gas chromatograph
- In **1960**, Shimadzu developed a vacuum quantometer, a device which served as a major stimulus to the steel industry
- In **1961**, Shimadzu created a remote-controlled X-ray fluoroscopy system
- **1968**: The European Headquarter in Germany was established
- In the **1970s**, Shimadzu increased its ties with China and countries in the Middle East. Exports to Singapore, Moscow, and other markets followed
- **1999**: Development of the world's fastest DNA sequencer
- **2002**: Shimadzu engineer Koichi Tanaka is awarded the Nobel Prize in Chemistry and Japan's Order of Cultural Merit
- **2003**: World's first diagnostic imaging system with a direct-conversion flat-panel detector
- **2010**: release of ground breaking UHPLC, GC and Spectroscopy systems
- **2012**: Release of high performance GCMS and LCMS TQ systems
- **2014**: Release of revolutionary Imaging mass spectrometry system

»It is the dose that makes the poison«

New ICPE-9800 series – Fast and reliable elemental analysis of drinking water

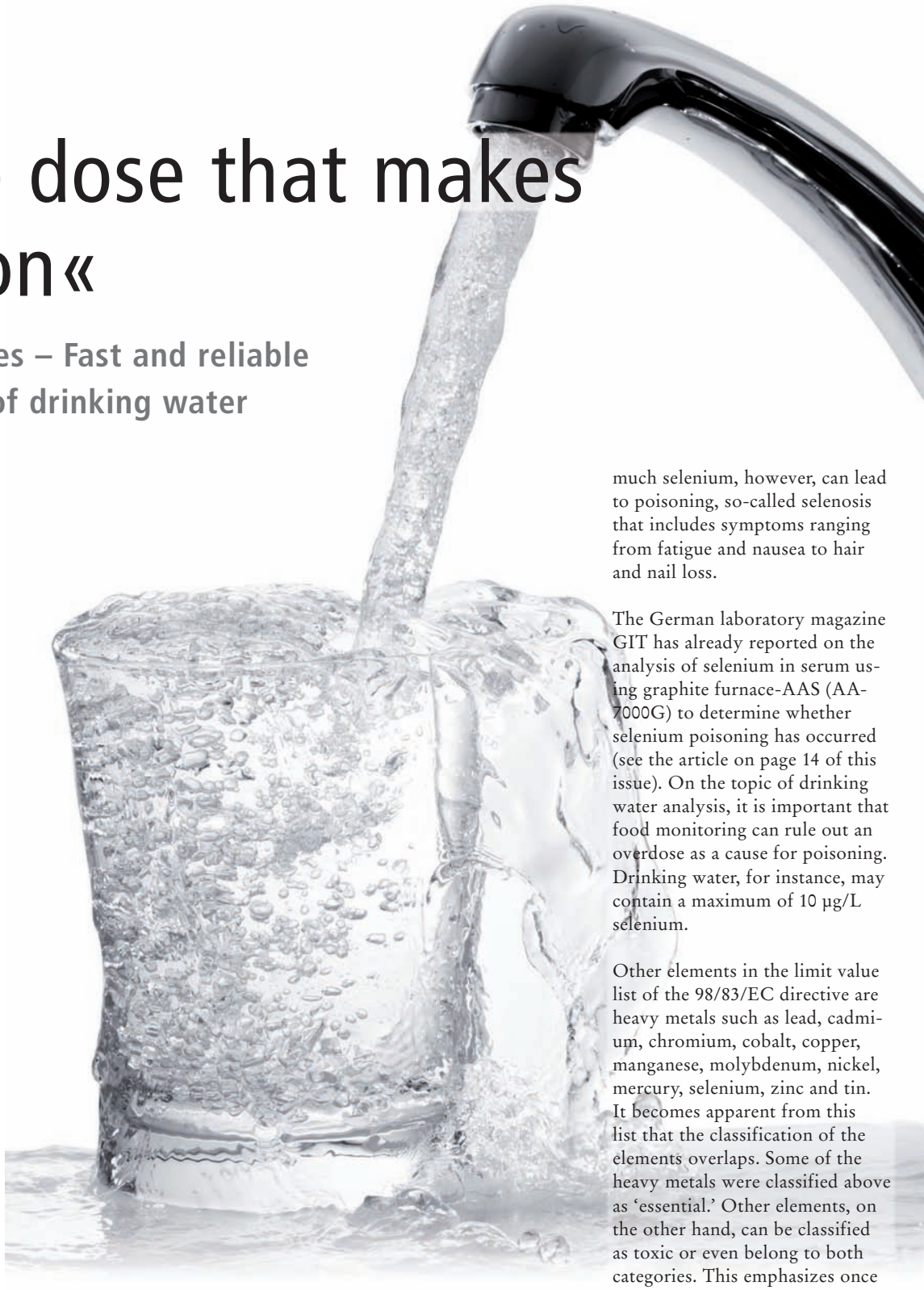

Essential to life, drinking water is the most important nutrient source. For an adult, the daily drinking water requirement is approximately 2 - 3 liters per day. While in some regions in the world it is still very difficult to provide and guarantee safe drinking water supplies, the situation in Europe appears to be very good. The next step is therefore to determine the quality of drinking water and to comply with specific standards, as not all water is considered healthy or could even be classified as potable water.

In the 98/83/EC Drinking Water Directive on the quality of water intended for human consumption, the European countries have specified when water is considered to be drinking water or when its consumption is prohibited. The testing criteria mentioned in this directive must be complied with and must be adopted into existing national law.

Some parameters in the 98/83/EC directive can be tested easily, for instance coloration. If a water sample tests negative, it can already be classified as questionable. But water that does not exhibit significant turbidity can also be harmful to humans.

Elements present in water

As a natural product, water contains many substances such as organic compounds or inorganic constituents. The term mineral water already points to some of these substances – essentially minerals such as calcium, potassium, magnesium and sodium. These inorganic nutrients are essential as the human body does not synthesize them, and they must therefore be obtained from a dietary source.

There are, however, many other essential elements in drinking water such as the trace elements chromium, cobalt, iron, copper, manganese, selenium and zinc. Other tentative candidates, whose exact functions as trace elements in the human body have not yet been conclusively investigated, could for instance be arsenic, nickel or tin.

For all these elements, the concentration plays a key role. For example, when selenium is missing, leads to a deficiency, and selenium-dependent enzymes that are present in almost every organ cannot perform their function. Too much selenium, however, can lead to poisoning, so-called selenosis that includes symptoms ranging from fatigue and nausea to hair and nail loss.

The German laboratory magazine GIT has already reported on the analysis of selenium in serum using graphite furnace-AAS (AA-7000G) to determine whether selenium poisoning has occurred (see the article on page 14 of this issue). On the topic of drinking water analysis, it is important that food monitoring can rule out an overdose as a cause for poisoning. Drinking water, for instance, may contain a maximum of 10 µg/L selenium.

Other elements in the limit value list of the 98/83/EC directive are heavy metals such as lead, cadmium, chromium, cobalt, copper, manganese, molybdenum, nickel, mercury, selenium, zinc and tin. It becomes apparent from this list that the classification of the elements overlaps. Some of the heavy metals were classified above as 'essential.' Other elements, on the other hand, can be classified as toxic or even belong to both categories. This emphasizes once more that the concentration is decisive.

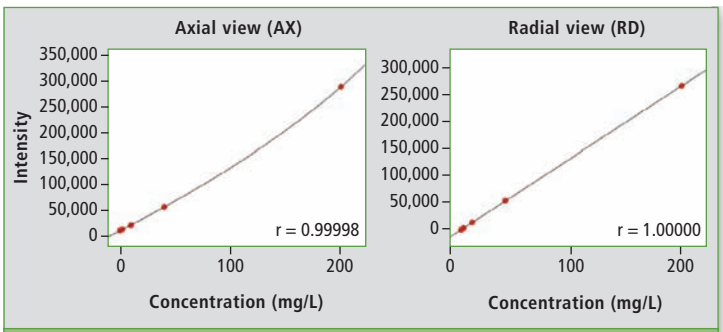

Figure 1: Radial plasma observation masks ionization interferences at high sodium concentrations (right) and the linear working range can be markedly extended

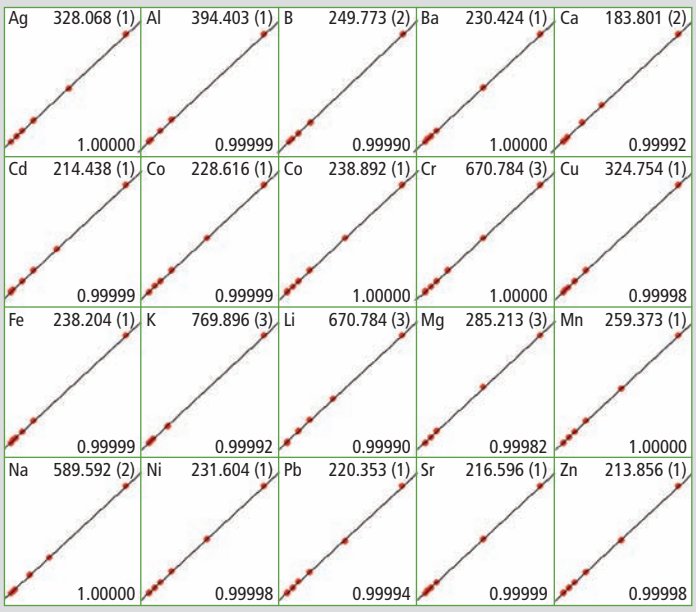

Figure 2: By Shimadzu's ICPE solution software all calibration curves can be obtained easily at first glance

Drinking water analysis

The elements specified in the 98/83/EC directive should be analyzed with a minimum of effort and within the shortest time possible. These elements, along with other important minerals, are listed in table 1.

When a large number of elements are to be determined, the new ICPE-9800 series proves to be particularly advantageous because it can determine all elements simultaneously. Of this series, the ICPE-9810 is suitable for the determination of ultra-trace concentrations of most of the elements mentioned. The ICPE-9810 is operated under axial plasma observation (AX). Since higher ppm-ranges, such as for sodium, are also of interest, radial plasma observation (RD) is required as well. The ICPE-9820 offers this combination of axial and radial plasma observation.

The exact effect of axial and radial plasma observation is shown in the example for sodium. The calibration series up to 200 mg/L is observed both axially (complete plasma) and radially (plasma section, from the side). The calibration curve under axial observation is not linear, as so-called ionization interferences can occur, especially at high concentrations of the main group 1 elements (e.g. sodium or potassium). These can be masked using radial plasma observation.

Results

The detection limits required according to the European 98/83/EC directive can be attained using the ICPE-9820. Figure 2 shows all calibration curves. Certified reference materials – drinking water samples with known content of the elements listed in table 1 – were also measured as unknown samples within one measuring sequence. Three different reference material samples (TMDW, trace metals in drinking water), supplied by High Purity Standards (North Charleston, SC, USA), were investigated.

The results in table 2 show that the certified concentrations were recovered within a short time and with very little effort. The elements mercury, arsenic, antimony and selenium can be measured sensitively when switching to the hydride vapour technique.

The ICPE-9820 series complies with the latest standards and can also be used in many different fields of analysis, for instance in the food or pharmaceutical industries as well as in the petrochemical industry.

Element[1]		98/83/EC directive		ICPE-9820	
		Limit value 98/83/EG [µg/L]	Detection limit [µg/L]	Detection limit [2] [µg/l]	Plasma observation
Al	Aluminum	200	20	2.5	Axial
As	Arsenic	10	1	2.0 (0.3*)	Axial
B	Boron	1,000	100	1.00	Radial
Ca	Calcium	– –	– –	90	Radial
Cd	Cadmium	5.0 [3]	0.5 [3]	0.20	Axial
Cr	Chromium	50	5	0.12	Axial
Cu	Copper	2,000	200	0.60	Axial
Fe	Iron	200	20	0.45	Axial
Hg	Mercury	1	0.2	2.0 (0.10*)	Axial
K	Potassium	– –	– –	15	Radial
Mg	Magnesium	– –	– –	18	Radial
Mn	Manganese	50	5	0.15	Axial
Na	Sodium	200,000	20,000	60	Radial
Ni	Nickel	20	2	0.45	Axial
Pb	Lead	10	1	0.90	Axial
Sb	Antimony	5	1.25	1.25 (0.15*)	Axial
Se	Selenium	10	1	2.0 (0.13*)	Axial

Table 1: The elements and their limit values specified in 98/83/EC, as well as the required detection limits of the analytical instruments. The detection limits specified for the ICPE-9820 refer to the present application.

[1] In addition elements that can be determined using the ICPE-9800 series can be included in the analysis (more than 70).

[2] Determined as 3-fold standard deviation of a natural sample with a low concentration of the element. The detection limits refer to the drinking water application and can be improved depending on the selection of the spectral line/application.

[3] The limit value in Germany according to the German Drinking Water Ordinance is 3,0 µg/L, the detection limit is at 0.3 µg/L.

[*] using the hydride vapour technique.

	CRM-TMDW[1] µg/L	ICPE-9820 µg/L	CRM-TMDW-A[1] µg/L	ICPE-9820 µg/L	CRM-TMDW-B[1] µg/L	ICPE-9820 µg/L
Al	120	117	125	121	125	124
B	n.c. [2]	– –	150	152	150	147
Ca	35,000	35,300	31,000	31,000	31,000	30,900
Cd	10	10	10	10	10	10
Cr	20	20	20	19	20	19
Cu	20	20	20	20	20	19
Fe	100	99	90	90	90	87
K	2,500	2,550	2,500	2,510	2,500	2,570
Mg	9,000	9,000	8,000	8,010	8,000	7,820
Mn	40	39	40	40	40	39
Na	6,000	6,160	2,300	2,240	22,000	22,800
Ni	60	57	60	58	60	57
Pb	40	38	20	20	20	18
Zn	70	68	75	73	75	75

Table 2: Recoveries of the elements that are contained in the reference material lie within the range of 100 ± 5 %

[1] The certified reference values are reported with an uncertainty of 0.5 - 2.0 %

[2] n.c. = not certified

For further information, please scan the QR code.

Further information on this article
• Applications

www.shimadzu.eu/shimadzu-news-2015

Animal kingdom suffering from plastic wastes

FTIR analysis of polymers in fulmars

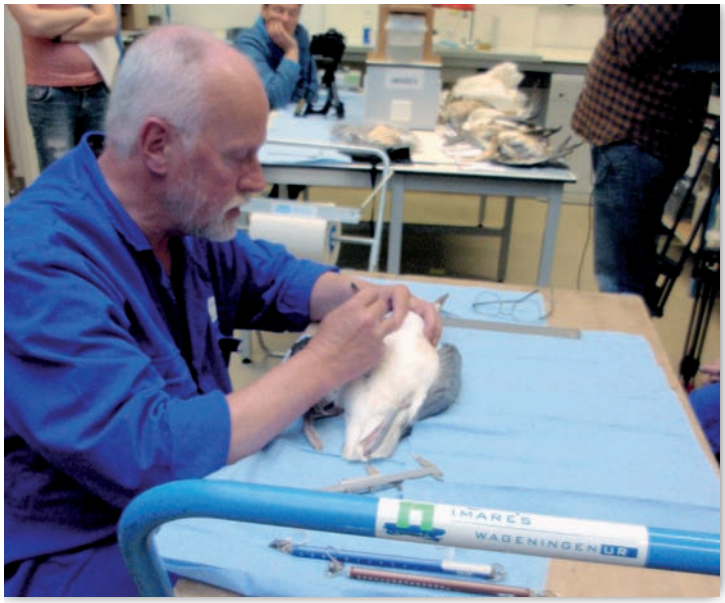

Figure 1: Dr. J.A. van Franeker during the workshop (2014) dissecting a young bird, whose stomach contents are shown in Figure 2

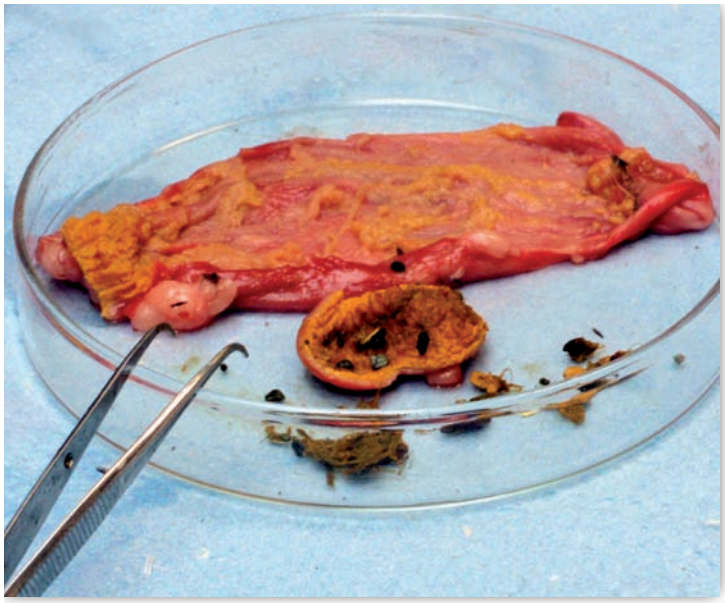

Figure 2: Stomach content of a fulmar, including many polymer particles in various sizes and appearances. For years this research has been carried out and recorded statistically by Dr. van Franeker.

In the autumn of 2014, the 'Fulmar Litter Monitoring' workshop* organized by IMARES (Institute for Marine Resources & Ecosystem Studies) took place on the Dutch island of Texel. The workshop focused on the analysis of stomach contents of dead fulmars (Fulmarus glacialis) that were found along the shores of the North Sea.

During the workshops, the participants under the guidance of Dr. Jan. A van Franeker (Figure 1) learned how to examine the birds externally and internally in order to categorize the animals in terms of age, gender and other important features.

After external inspection, the bird is examined internally. For the application described here, the stomach content of the bird is of interest. The stomach of a fulmar extends virtually over the entire body of the bird, as it has to digest whole fish. The stomach is actually subdivided into two stomachs: the proventriculus and the gizzard. Predigestion takes place in the proventriculus and hard parts are ground in the gizzard and converted to food (Figure 2).

The North Sea countries have recognized the threat posed by plastic waste since many years, and their goal is to reduce the concentration of plastics in the ocean to such an extent that most fulmars will contain less than 0.1 g of plastic in their stomachs (i.e. not more than 10 % of the birds containing more than 0.1 g). These values are not statistically attained in the 5 regions of the surrounding North Sea coastlines (Figure 4).

Although fulmars feed on anything that swims, such as fish and squid, the birds also consume plastic wastes. They mistake plastics for food. Plastics can accidentally be taken in during fishing or the plastic can already be contained in the fish they eat. The fulmar fishes on the ocean surface up to a maximum diving depth of 2 m, where mainly light polymers such as polyethylene and polypropylene are present.

Plastic waste is very diverse in appearance. This is why an optical categorization has been introduced, for example industrial,

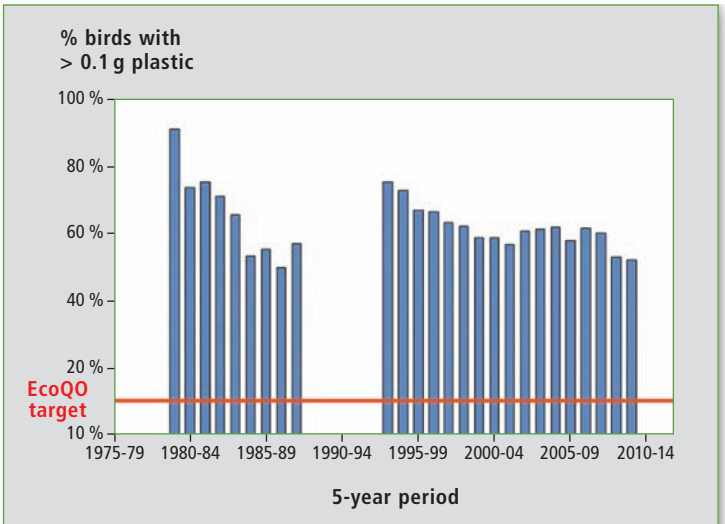

Figure 3: Trend analysis (5-year summary) for the occurrence of plastics in the stomachs of fulmars in the Netherlands. The trend shows a slight drop over the years, but it is still significantly far higher than the EcoQO target which is to reduce the percentage of birds with more than the limit value of 0.1 g of plastic in their stomachs to below 10 %.

applied/used, non-plastic and pollutant.

Exact statistics for fulmars in the Netherlands from 2009 to 2013 were: 227 fulmars were examined, 94 % had plastic materials in their stomachs. The mean value of material per stomach was 28 particles with a total weight of approx. 0.3 g. The critical EcoQO value of 0.1 g plastic was exceeded in 52 % of the birds [1].

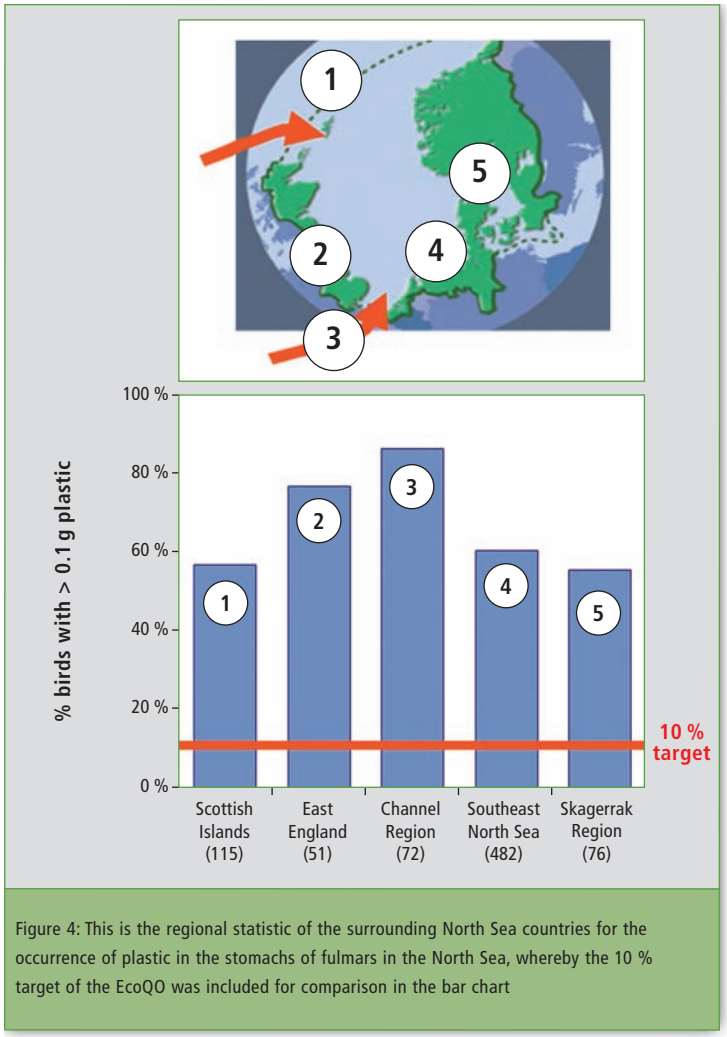

Figure 4: This is the regional statistic of the surrounding North Sea countries for the occurrence of plastic in the stomachs of fulmars in the North Sea, whereby the 10 % target of the EcoQO was included for comparison in the bar chart

What does 0.3 g of plastic mean?

This amount may seem very little – but in terms of the body weight of a fulmar, 0.3 g of plastic would correspond to 20 g of plastic in a person weighing 70 kg, i.e. one fifth of a bar of chocolate (see figure 5).

Why FTIR?

Using this infrared spectroscopic measuring technique, all types of materials and their appearances can be measured non-destructively, including plastics from fulmar stomachs. When the FTIR system (IRAffinity-1S) is equipped with a single-reflectance ATR unit (Quest™), the sample can be measured directly. Sample preparation merely involves drying the sample with paper after briefly rinsing with water. Under this condition, the polymer is expected to be sufficiently clean.

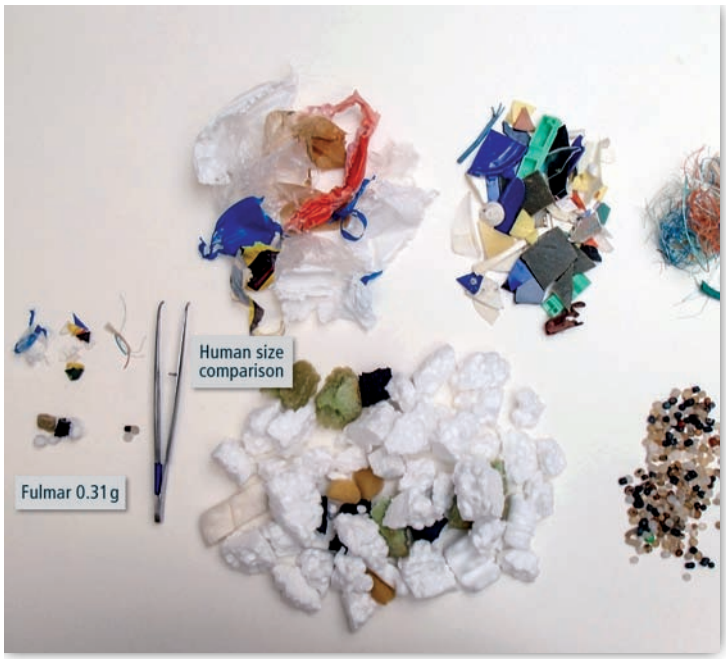

Figure 5: Comparison of the amount of plastic in a bird's stomach (left, North Sea, mean value) with the extrapolated volume corresponding to the size of a human. For a person weighing 70 kg, this is more than 20 g.

An ATR unit enables surface measurement, which in this case is carried out at a penetration depth of approx. 2 µm. The sample is held in contact with a diamond prism and pressed against it using an anvil. The infrared spectra measured assist in the identification of the polymers, all within seconds. The measurement time and analysis was one minute. FTIR-ATR is therefore a suitable method for measuring large sample amounts (for instance also for monitoring).

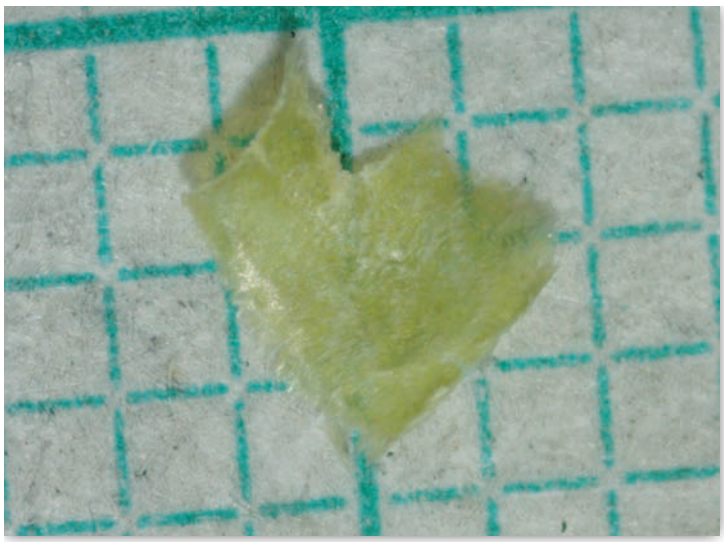

Figure 6: FTIR spectrum of a thin foil, which was measured using the Quest diamond single-reflectance unit

Measuring results

A major problem in the analysis of natural field samples is false analysis. This is explained using a thin piece of foil.

The spectrum obtained from the piece of foil was analyzed further using a polymer library. The result of the search identified the material as a polyamide (nylon). A purely visual comparison of the spectral structure, as well as the library search result with a hit of 700 (good agreement over 900) clearly shows that no good correlation was obtained.

When expanding the library with the know-how on this foreign sample, the hit rate was better and more reliable. For an improved analysis, many additional facts are needed, for instance: what does the bird eat, what is the consistency of the gastric fluid and so on.

To better classify spectrum (Figure 7), two additional reference spectra (fish skin ⏵

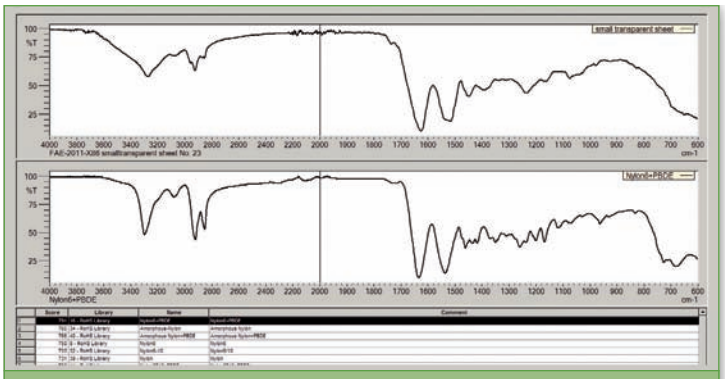

Figure 7: Analysis of a thin foil using infrared spectroscopy and library identification. (False result). The material is not Nylon.

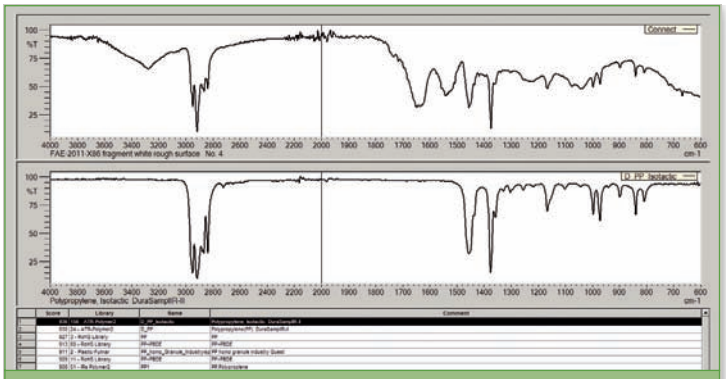

Figure 8: Library search of an infrared spectrum of a white fragment with rough surface. Here, the correct polymer polypropylene was found. The additional bands can be assigned to protein and fat.

and also stomach fat) are required (Figure 8). When combining the fat spectrum of the fulmar with the fish skin spectrum, the spectrum left is obtained.

The second example shows a fragment with the description 'white with rough surface.'

The library search has therefore led to the correct result. Polypropylene constitutes part of the spectrum. So do proteins and small amounts of fat. All three contribute to the spectrum. The polymer is found with a hit accuracy of 930 out of a maximum of 1.000.

Discussion of the measured results

Materials that have become enriched in fulmar stomachs can be investigated using infrared spectroscopy. Surface analysis enables the determination of materials at a layer depth of 2 µm. Depending on the 'history' of the particle, it can exhibit a certain 'roughness' in which digestion fluids can collect. Due to the fatty foods, many of the samples have been found to contain fat which accumulates in the pores. Should these samples be rinsed with a fat remover, the infrared spectra of the cleaned surfaces could lead to a higher hit rate. Knowing this enables rapid screening of the particles on non-cleaned surfaces.

Authors

Dr. J. A. van Franeker, IMARES Wageningen UR
Albert van Oyen, Carat GmbH
Marion Egelkraut-Holtus, Shimadzu Europa GmbH

References

[1] Fulmar litter EcoQO monitoring in the Netherlands – Update 2012 and 2013, J.A. van Franeker, S. Kühn, E.L. Bravo Rebolledo, A. Meijboom, Report number C122/14, IMARES Wageningen UR

Further information on this article

- Dossier – Plastic waste and marine wildlife
- Carat GmbH
- IMARES

www.shimadzu.eu/shimadzu-news-2015

PRODUCTS

Small yet high-performance

New UV-VIS spectrophotometer UV-1280

Organic and aqueous solutions, biological samples, optical materials such as filters or foils and much more – the new UV-VIS spectrophotometer UV-1280 (Figure 1) enables spectral analyses for a wide range of samples. The compact system with a spectral bandwidth of 5 nm allows measurements with high stability in a wavelength range of 190 - 1,100 nm.

The UV-1280 has a very small footprint. It is easy to operate using function keys and the large LCD monitor which also displays the on-board software. The following functions and programs are provided as standard:

UV-1280

1. photometry
2. spectrum
3. quantitative analysis
4. kinetics
5. time-scan measurement
6. multicomponent analysis
7. DNA/Protein quantification.

In addition, the UV-1280 enables instrument validation. It tests the following instrument parameters: wavelength accuracy and repeatability, stray light, photometric accuracy, photometric repeatability, baseline flatness and baseline stability, as well as noise level.

The wide application range is supported by a comprehensive range of accessories which is used individually in the sample compartment. Via the USB connection, data can be copied directly in the USB memory and evaluated using spreadsheet software. A printer with USB-I/F interface can also be connected directly to the UV-1280.

New milestone in ICP-OES technology

ICPE-9800 spectrophotometer series reduces operating costs

For more than 30 years, inductively coupled plasma (ICP) has been used commercially as an excitation source for optical emission spectrometers and has become an indispensable tool for daily routine applications.

Since the introduction of the first sequential ICP-OES spectrometer ICPQ-100 in 1977, Shimadzu has been a driving force in technical innovation. The ICPS-8100, for instance, features exceptional light intensity while achieving high resolution. The optical systems with 1-meter monochromator have defined standards in this instrument class. With the launch of the ICPE-9000 in 2005, a simultaneous system with vacuum optics and minitorch was introduced.

The new ICPE-9800 series is a follow-up to this success story and sets a new milestone in ICP-OES instrument technology.

The new simultaneous spectrometers in the ICPE-9800 series are equipped with vacuum high-performance optics and use a 1,024 x 1,024 pixel CCD (charge-coupled device) detector. This system allows simultaneous acquisition of spectral data over the entire wavelength range of 167 to 800 nm without exception, i.e. all element information and wavelengths are available to the user at any time.

High-performance optics

The new series includes two spectrometers:

- the ICPE-9810 with vertical orientation of the minitorch and axial plasma observation for the highest possible sensitivity
- the ICPE-9820, also with vertical orientation of the minitorch but with axial and radial plasma observation.

ICPE-9820

This allows the ICPE-9820 to carry out analysis of samples containing low-concentration elements (axial) and high-concentration elements (radial) within one sequence.

The intelligent ICPEsolution software enables automatic wavelength optimization as well as correction of interferences. Assistant functions help to develop methods and to evaluate the results.

Minimum operating costs

In the new ICPE-9800 series, there was particular emphasis on minimizing operating costs as well as on high performance. For instance, argon consumption is reduced to 10 L/min due to the minitorch technology. The vacuum optics do not require purging of the optical tank with argon or nitrogen, as is common in many spectrometers.

Moreover, the energy-saving Eco mode enables further reduction of argon and energy consumption during standby operation between measurements. Using 99.95 % pure argon instead of the commonly used 99.999 %, only required for purging the optics, is an additional savings potential. In this way, up to 20,000 Euro can be saved over a three-year operating period.

The accessories program includes a wide selection of pneumatic nebulizers, nebulizer chambers and ultrasonic nebulizer for various sample materials. Combining with autosamplers such as the ASC-9800 or the ASX-520 enables fully automated multi-element analysis. Through the use of the ASXPress PLUS sample introduction system, measuring times of less than one minute can be achieved for the highest possible sample throughput and reliable results.

Insights on molecular level

iMScope *TRIO* with revolutionary technology

iMScope *TRIO* – Imaging Mass Microscope

In recent years, imaging mass spectrometry (imaging MS) has received increased attention through a variety of applications. This fairly new innovation in mass spectrometry allows spatial assignment of analytes as well as their identification. The sample – for instance, a tissue section – is analyzed using mass spectrometry at specified locations in a grid. The mass spectra of the individual points are subsequently combined via dedicated software into one image (MS image) which represents the distribution of individual substances within the sample. This way, the occurrence of certain molecules at specific locations can be compared with morphological abnormalities.

With the iMScope *TRIO* (Figure 1), Shimadzu offers a worldwide unique instrument for imaging mass spectrometry. The iMScope combines an optical microscope and a high-resolution mass spectrometer in one single instrument. This allows direct comparison of the MS image with the microscopic image. Substances from samples that were microscopically examined cannot only be identified directly, but their spatial distribution within a tissue can also be determined.

World's best spatial resolution

The optical microscope can acquire images in epi- and trans-illumination, as well as fluorescence images (up to 5 optional wavelengths). The analytes are ionized via MALDI (Matrix-Assisted Laser Desorption/Ionization) at atmospheric pressure.

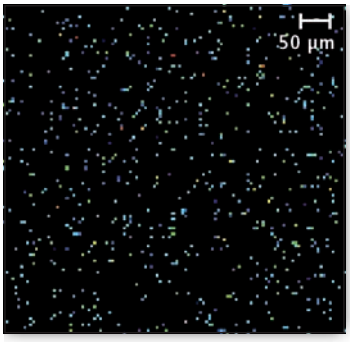

Figure 1a: MS/MS image of quercetin (m/z 269.2 → 224.97)

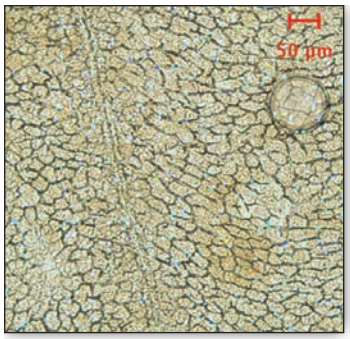

Figure 1b: Overlay of the MS/MS image with the optical image

The solid-state laser used for this purpose can scan the sample with a variable diameter of 5 to 200 µm. This results in a maximum resolution of the MS images of 5 µm which is currently the world's best spatial resolution that can be achieved.

The ionized molecules are subsequently analyzed using the integrated ion-trap time-of-flight (IT-TOF) mass spectrometer. The high-resolution system can also carry out MSn analyses which enables identification as well as structural elucidation of the target analytes. Furthermore, MS/MS analysis increases the sensitivity due to a better signal-to-noise ratio.

With an analysis speed of six pixels per second, MS images can be acquired rapidly. This way, acquisition of 250 x 250 pixels (62,500 pixels) takes less than three hours. The possibility of exchanging the MALDI source for an ESI (Electrospray Ionization) source further increases the flexibility of the system and the mass spectrometer can also be used for the analysis of liquid samples.

Large application bandwidth

There is a wide range of possible application areas, such as the analysis of biomarkers, active substances and their metabolites in tissues, the distribution of substances in foods and plants, but also the analysis of micro-defects or minute contaminations in synthetic materials. In general, the iMScope *TRIO* is used in innovative Research & Development.

The following example shows which additional information is

gained from the comparison of an optical image with an MS image. A rat liver section was treated with quercetin and used for analysis. The MS image (Figure 1a) alone shows an apparently random uniform distribution of quercetin over the entire sample. After overlaying with the microscope image (Figure 1b), a correlation between the localization of the molecule and the structures within the investigated liver tissue can already be visualized. Magnification of the overlayed image (Figure 3) clearly shows that all the detected quercetin molecules are exclusively localized in the intracellular space or on the cell walls and not inside the cells.

The use of a larger laser beam diameter would have resulted in a loss of spatial information about the localization of quercetin within the tissue. A precise allocation to the intracellular space or the cell membrane would not have been possible.

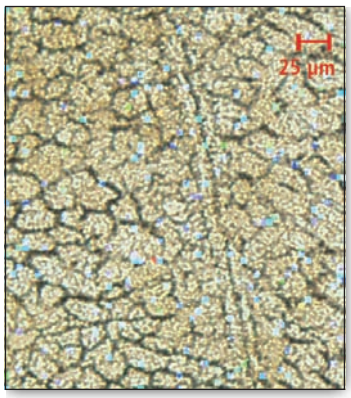

Figure 2: By enlarging the superimposed image, it can be seen that quercetin is localized in the intracellular space and not inside the cells

Resolution is application dependent

Depending on the investigated object, a medium or high spatial resolution is required. In order to study the localization within larger tissue structures, a medium resolution is sufficient, whereas localization on the molecular level requires the highest possible resolution.

High resolutions can be used to determine the distribution of drugs in microstructures or the accumulation of their metabolites.

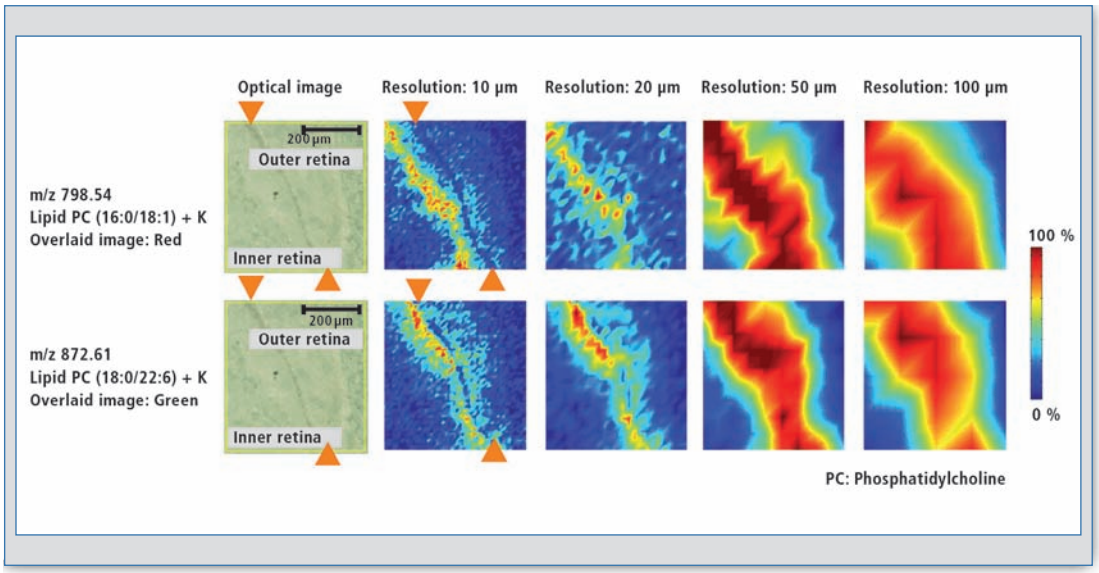

Figure 3: Microscopic image of the retina as well as MS images for two different lipids at resolutions of each 10 µm, 20 µm, 50 µm and 100 µm

For the investigation of various lipids that are present in the retina of the eye, a higher resolution of 10 µm was selected. The microscopic image (Figure 4) shows the retinal pigment epithelium as a dark band that separates the inner from the outer retina. MS images (Figure 4) of two different lipids (m/z = 798.54 und m/z = 872.61) were acquired using several resolutions (10 µm, 20 µm, 50 µm und 100 µm). The outline of the retinal pigment epithelium only can be recognized at a resolution of at least 10 µm. At a lower resolution this outline is lost.

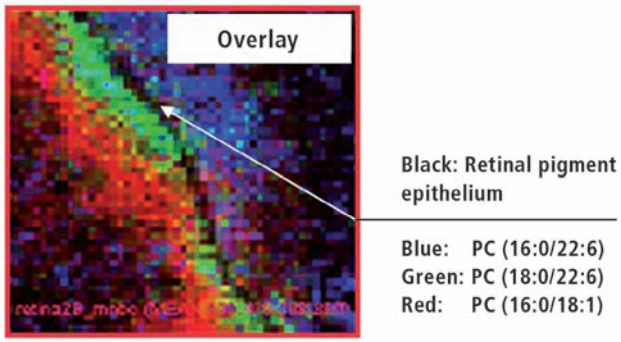

Figure 4: Overlay of the MS images from three different retinal lipids

Software for data acquisition and analysis

The 'Imaging MS solution' software specifically developed for the iMScope *TRIO* is used for data acquisition as well as for data analysis. The software allows the overlaying of several MS images (Figure 5). The high resolution of the MS images allows for accurate assignment of the three investigated lipids. While PC (phosphatidylcholine, 16:0/22:6) exclusively occurs in the outer retina, PC (18:0/22:6) can be found directly adjacent to the retinal pigment epithelium in the inner retina, and PC (16:0/18:1) even further inside the retina.

Additional tools for statistical data analysis are Hierarchical Cluster Analysis (HCA), Region of Interest Analysis (ROI) and Principal Component Analysis (PCA).

Matrix deposition without delocalization

To obtain MS images with maximum spatial resolution, sample preparation is very important, next to an excellent performance of the mass spectrometer. The matrix required for ionization is conventionally dissolved in liquid and sprayed or spotted onto the sample. As a result, there is always a risk that the target analytes will dissolve in this liquid and diffuse inside the sample. This will lead to the situation that despite using instruments, which are capable of high-resolution sample analysis, the sample no longer yields such a high resolution.

With the iMLayer, Shimadzu therefore offers a device for matrix application with which this effect cannot occur. The matrix is deposited via a sublimation process, whereby a thin layer of very small matrix crystals is applied, and delocalization of analytes cannot occur. In combination with the iMLayer, the iMScope offers a unique and complete solution for sample preparation, acquisition and overlay of optical and MS images with the world's best spatial resolution, as well as (statistical) data evaluation via imaging MS solution software.

The secrets of a Swiss watch

»In our lab we R.E.A.C.H. the very secrets of matter«

A few kilometres south of the French border, the city of La Chaux-de-Fonds is located in the French-speaking part of Switzerland in the Jura mountains. The city is the most important center of the watch making industry in the country and was added to the World Patrimony of UNESCO. It is home to Metallo-Tests SA, and no wonder, since the company as an independent laboratory accredited for Swiss testing focusses on materials and elements testing for the watch-making industries. Besides this key area, Metallo-Tests serves the medical industry, micro-electronics, telephony, writing instruments, leather goods and accessories, eyewear, toys, packaging, automotive and environment.

Figure 1: HPLC *Nexera* with Photodiode Array detector

Metallo-Tests SA aims to cater perfectly to the constraints imposed by the introduction of new laws or standards (especially in chemical analysis) and the increase of market requests. For over thirty years, the company continues to expand by investing regularly in advanced equipment. The example of a wristwatch demonstrates Metallo-Tests' core competencies.

Biocompatibility and REACH compliance of a wristwatch

REACH (Registration Evaluation Authorization of Chemicals) is a European regulation concerning all chemicals manufactured in or imported into Europe. Chemical substances must be registered and their potential risk for health or environment are evaluated. If they are carcinogenic, endocrine disruptor or organic pollutant they can be restricted (SVHC = Substances of Very High Concern)

A watch is made up of many elements that must meet the criteria for biocompatibility and the REACH Regulation of the European Union to prevent allergy in the consumer or legal non-compliance problems with the country in which the watch is sold. A bracelet can be made of leather, rubber or steel. Depending on the constituent materials, the substances of restriction will be different.

Leather straps – Chromium VI

For example, the majority of leather straps are tanned with chromi-

um salts (III). Poor control of the tanning process can cause oxidation of Cr III to Cr VI, the latter being carcinogenic and mutagenic. It is therefore limited to 3 mg/kg in Europe for leathers which come into contact with skin [1].

Extraction is carried out according to ISO 17075. After discoloration of the extraction solution by a passage through a C-18 cartridge, a reagent is added to form a pink complex with Cr VI. A dosage at 540 nm allows the content of Cr VI to be determined. This analysis is executed with the compact UV-2600 universal, research-grade spectrophotometer that can be used in a wide range of fields and expanded easily to suit the measurement objective.

Formaldehyde

The leather straps are usually designed with a finishing to be more resistant to environmental constraints such as sweat, humidity and cosmetics. Treatments to improve their strengths may contain formaldehyde which can be irritating and is recognized as carcinogenic. It is restricted in many countries at 75 mg/kg [2].

Extraction is carried out according to ISO 17226-1 and assay is performed on a *Nexera* UHPLC with Photodiode Array detector at 360 nm.

Short-chain chlorinated paraffin (SCCP)

With these leathers, the presence of short-chain chlorinated paraffin SCCP is also verified in accordance with ISO/DIS standard 18219. These waxes are generally derived from greasing treatments used to prevent them from drying out. The use of SCCP is banned in Europe since they pollute the environment [3]. These SCCPs can also be found in plastics or rubbers where they are used as flame retardants. After extraction, they are assayed on a GCMS-QP2010 gas chromatograph mass spectrometer with NCI detector to increase sensitivity.

Plastics and rubber straps

Bracelets made of rubber or plastic can be of diverse nature (FKM, HNBR, NBR, PVC, silicone etc.). Analysis on Shimadzu's FTIR spectrometer IR Prestige-21 with

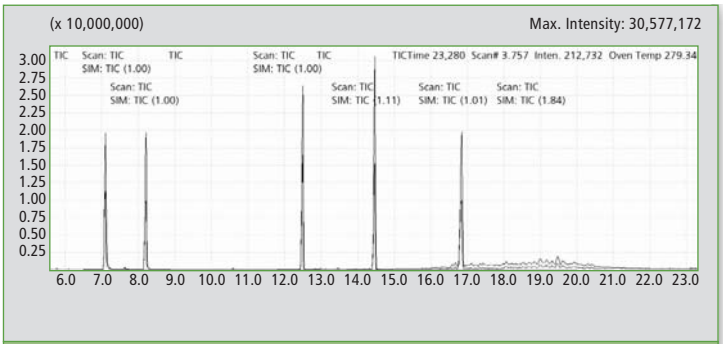

Figure 3: GC-MS spectrum of phthalates mix (DiBP, DBP, BBP, DEHP,DnOP, DiNP/DiDP)

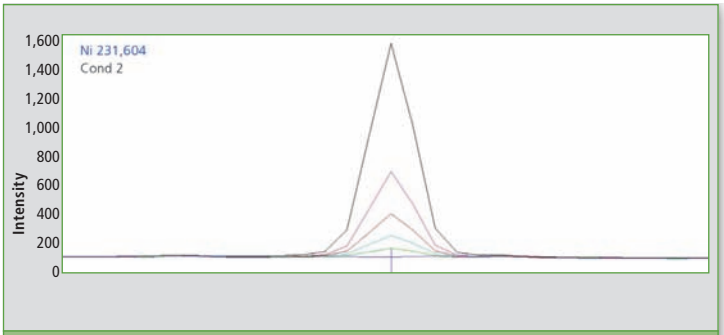

Figure 4: ICP-OES spectrum of Ni at concentrations between 100 and 2,500 µg/L at 231 nm

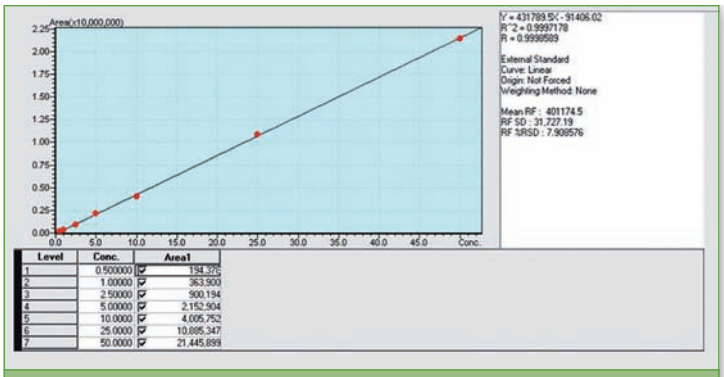

Figure 2: Calibration curve of DEHP (Di-[2-Ethylhexyl]phthalate) softener with GCMS-QP2010

ATR cell enables a rapid diagnosis to determine which family the polymer belongs to. This analysis also verifies the absence of polymer degradation after aging by environmental testing, such as ozone, sunlight exposure, heat and humidity, sweat contact or oxidative vapors. These tests simulate surrounding conditions the bracelet will be submitted to.

Plasticizers

In case where a watch contains rubber or plastic, there is a potential risk in the presence of plasticizers such as restricted phthalates. Some phthalates are subject to authorization [4] because they are classified as endocrine disruptors. One of the most used restricted softeners is DEHP (Di-(2-ethylhexyl) phthalate, CAS No. 117-81-7). Phthalates are extracted according to EN 15777 or ISO 16181. They are then measured by GCMS-QP2010 with EI detector.

Metals

Where metallic elements in contact with the skin contain nickel, such as AISI 316L stainless steel as case or clasp, a nickel release test is required. Nickel allergy affects a large percentage of the population (nearly 13 %, largely female). Before being sold, the parts to be in direct and prolonged contact with the skin are checked according to EN 1811. Their nickel release must be in compliance with REACH [5]. The tested components of the watch are immersed in an artificial sweat solution for one week and the amount of nickel released is measured by ICPE-9000 inductively coupled plasma emission spectrometer at the most sensitive wavelengths of nickel, 221.6 and 231.6 nm.

Author

Dr. Sandra Wermeille
Metallo-Tests SA
La Chaux-de-Fonds, Switzerland
www.metallo-tests.ch

Legal references:

[1] LBFG Deutschland und REACH, Annex XVII
[2] Japanese Law 112 und GB 20400/2006 China
[3] Reg. (EC) No. 850/2004 (Act on Persistent Organic Pollutants)
[4] REACH, Annex XIV und List of SVHC (Substances of Very High Concern)
[5] REACH Annex XVII, Entry No. 27

METALLO TESTS SA
LABORATOIRE D'ANALYSES CHIMIQUES
CARACTÉRISATION DES MATÉRIAUX
TESTS DE VIEILLISSEMENT MÉCANIQUE ET CLIMATIQUE
CONSULTING, CONTRÔLES, HOMOLOGATIONS

Selenium in blood serum

Atomic absorption spectroscopy for trace analysis

Blood or serum analysis can help in the diagnosis of numerous diseases and is also used to investigate possible excessive or insufficient supplementation with vitamins or trace elements. Blood serum is a difficult analytical matrix since it contains many different components, and serum analysis is therefore a major challenge. Atomic absorption spectroscopy offers a reliable and robust analysis method.

Instrumental analysis is an important diagnostic tool in the analysis of blood or blood serum. Many causes of disease can be determined from blood composition and can be treated accordingly. In addition to its many main components, blood also contains substances that the human body needs only in minute amounts. One of these substances is selenium.

Selenium is an essential trace element for the human organism. This means that the body only needs selenium in trace amounts. The selenium concentration in serum lies in the range of about 50 - 120 µg/L. Selenium deficiency occurs below this range and may cause a variety of problems. An excess of selenium is, however, toxic. The margin between selenium deficiency and a toxic concentration is very narrow. It is therefore important to determine the selenium concentration in blood and to monitor any additional selenium intake closely.

How atomic absorption spectroscopy works

Atomic absorption spectroscopy (AAS) with graphite furnace has been proven to be successful in the analysis of trace elements in serum. The advantages of this system are the high detection sensitivity (measuring range in the lower µg/L range), small sample volume required (10 - 20 µL) and the relatively low sensitivity to difficult matrices.

In order to operate an atomic absorption spectrometer, special lamps are required that contain the specific element to be analyzed – selenium determination therefore requires a selenium lamp. The selenium in the lamp is excited in such a way that it emits selenium-specific light.

The element-specific light is directed via a special mirrors through an optical path in which a so-called atomization unit is placed. In trace analysis, a graphite furnace atomization unit is used. This furnace includes a tube of about 3 cm in length made of compressed graphite. After passing through the graphite tube, the element-specific light is directed by other optical parts onto a photomultiplier which measures the incident light.

For the analysis, an aliquot of the sample (approx. 20 µL) is injected into the graphite tube and heated electrothermally. First, the solvent is evaporated and the remaining sample components are ashed. In a so-called atomization step, the sample is subsequently irradiated with enough energy to convert the sample components into many free excitable ground-state atoms of the respective element. In the ground state, atoms absorb energy from light emitted by the lamp. The system measures the light intensity attenuation (absorption) during the atomization phase (atomic absorption).

During atomization, temperatures of up to 3,000 °C are generated. To protect the graphite tube from oxidation (by atmospheric oxygen), a small continuous stream of argon is directed through the tube. The argon gas flow also focuses the resulting atomic cloud. The measuring range for selenium lies at about 2 µg/L to 25 µg/L (LOD < 0.5 µg/L) for sensitive systems (AA-7000G).

Various graphite tubes are available for graphite-furnace AAS. For serum analysis, graphite tubes with an omega-shaped platform have proven to be successful as they heat the sample uniformly.

Sample volume	Water added	Standard added (Selenium concentration 30 µg/L)	Palladium modifier added	Resulting selenium addition
10 µL	10 µL	0 µL	5 µL	0 µg/L
10 µL	5 µL	5 µL	5 µL	7,5 µg/L
10 µL	0 µL	10 µL	5 µL	15 µg/L

Table 1: Composition of the sample injection for the individual measuring points and the resulting concentrations of the selenium addition

Figure 1: The images show a graphite tube in the optical beam before and during the injection (total of 25 µL). It is important that the sample is carefully and 'reproducibly' placed in the tube.

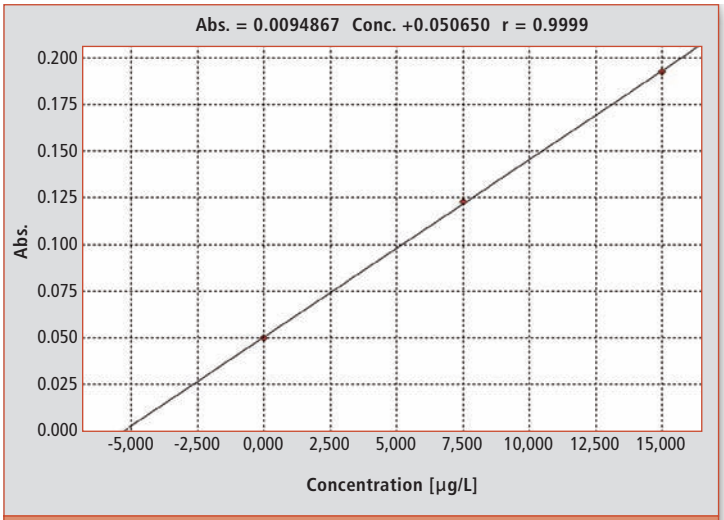

Figure 2: The graph shows the evaluation function according to the standard addition method (r = 0.9999)

Sample preparation

In addition to water (> 90 %) and soluble substances that occur naturally in blood, serum contains mainly proteins (about 7 %). Because of the high viscosity and the organic matrix (proteins), the serum sample is diluted at a ratio of 1:10 with ultrapure water. To further reduce the viscosity of the diluted sample, a surfactant (Triton X) is added to the dilution. This dilution can be placed directly in an autosampler vial for subsequent analysis. Due to the dilution factor (factor 10), the working range of this analysis is about 20 µg - 250 µg per liter of serum.

Temperature program

Selective, straightforward and sensitive analysis using graphite-tube AAS requires an adapted and optimized temperature program. First, the water must be evaporated slowly without splashing the sample in the graphite tube. The interfering organic substances are then ashed at temperatures up to 1,100 °C.

Selenium has a boiling point of 685 °C, and suitable measures must be taken to prevent lower measurement values. Injecting a small amount of palladium nitrate solution will suffice for this purpose. This can be programmed and carried out automatically via an autosampler.

The palladium modifies the selenium in such a way that it will only evaporate at higher temperatures and is therefore not volatile at higher drying temperatures such as 1,100 °C. The atomization step then takes place at 2,500 °C and needs just a few seconds. Absorption measurement also takes place during this time span.

Calibration

In graphite-furnace AAS, absorption is recorded along the time-axis during atomization. This results in a peak, whose height or area is used for calibration as a measure of concentration. For evaluation, external calibrations are typically used.

For difficult matrices such as blood serum, the standard addition method has become an established evaluation method. The sample is mixed with a standard solution in various ways and measured afterwards (Table 1, Figure 2). In this way, sample measurements in different concentration levels are obtained in which the individual matrix interferences of the sample are optimally taken into account.

When the measurement parameters (height or area) are plotted against the added selenium concentrations, the graph shows the sample concentration on the negative x-axis. In this way, each sample obtains its own internal evaluation function. The injection sequence is fully programmable and can be carried out using an autosampler. The user only has to fill the sample vials and provide the standard addition solution and the modifier. Evaluation of the results also takes place automatically.

Measurement example

Two certified sera with different concentration were tested for method development. The results and the standard deviation were obtained after three injections for each concentration level (Fig. 3, Tab. 2).

Conclusion

It is anything but easy to analyze trace elements in difficult matrices such as blood serum. A robust measurement system with an optimized furnace program, appropriate equipment and a suitable data evaluation method can make such specialized analytics available for routine analyses.

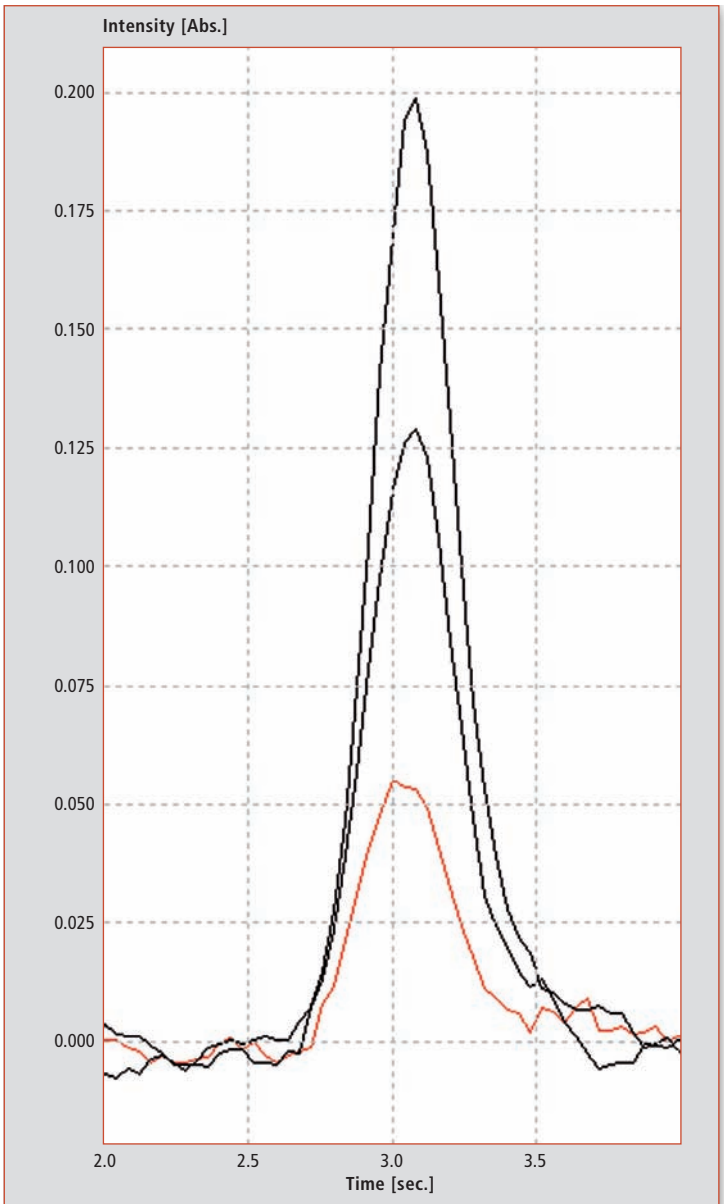

Figure 3: Peaks of three injections (red = sample without addition, black = both injections with different amounts of selenium). The y-axis shows the absorption versus time in seconds (x-axis).

Read for you
in G.I.T. Labor-Fachzeitschrift 8/2014

Serum	Specifications in accordance with analysis certificate			Results Shimadzu AA-7000G			
Sample	Measured values	Analyt. uncertainty*	Acceptable range	Measured values	RSD [%]	SD [µg/L]	Final result
Serum L-1	107 µg/L	100 - 114 µg/L	93 - 121 µg/L	107	3.92 %	4	107 ± 4 µg/L
Serum L-2	157 µg/L	150 - 164 µg/L	143-171 µg/L	158	4.00 %	6	158 ± 6 µg/L

Table 2: Certified reference sample concentrations (Sero, Norway) and related statistical data for results recovery (confidence interval/acceptance range) as well as analytical results of the AA-7000G (*95 % confidence interval)

Testing wine bottles

Combining UV and EDX – Non-destructive quality control, fast and simple screening method

Figure 1: Two wine bottles of different glass color were of interest. The green bottle on the left is referred to as an old wine bottle and the green-blue bottle on the right as a new wine bottle.

Some beverages are sensitive to light and can lose color and vitamins. This is why they are distributed in colored glass bottles to protect them from the influence of light. The color and shape of bottles are often part of the sales strategy to attract the attention of buyers. As the production of glass bottles requires much energy, recycling of glass is worthwhile. In Germany, recycling is promoted via the 'Green Dot' system. Used glass bottles are collected in separate containers for white, brown and green glass, and this multitude of colors is a challenge. How to handle blue glass or bottles that are neither brown nor green, but appear milky?

Colors are subjective, but they can also be characterized objectively using color tables. Spectroscopic methods such as UV-VIS spectroscopy can help. Depending on the desired quality of the end product, higher or lower percentages of recycled glass are being used in glass production. The base material silicon dioxide is mixed with coloring oxides. The oxides are used depending on the desired specifications (color) of the end product.

In white glass, for instance, iron oxide causes interference which makes the glass appear slightly green. If the color should be more intense, chromium oxide is added and the glass turns into more intense green. Brown glass contains manganese oxide and iron oxide. A variation of oxides results in different colors. To be able to limit the immense number of color shades, oxides of complementary colors are added to decolorize the glass.

It is therefore interesting to know the composition of the glass granulates before smelting and, with this knowledge, to add further oxides if necessary. A fast method to determine this composition is elemental analysis with an energy-dispersive X-ray fluorescence spectrometer (EDX). This technique enables direct non-destructive analysis of the material to determine its elemental composition. The technique provides information of the main elements and interfering elements in glass production.

While glass consists to a large extent of SiO_2, it is also possible to determine iron (Fe), manganese (Mn) and chromium (Cr) in addition to the silicon (Si) signal.
A traditional glass is made of lead crystal which contains lead oxides. The element lead (Pb) is also included in the analysis spectrum of the EDX systems and is in addition subject to the RoHS (Restriction of Hazardous Substances) directive.

The experiment presented here discusses the end product wine bottle. The intention is to analyze the bottle non-destructively. This is possible using UV-VIS spectroscopy as well as the EDX system. The sample compartments in both instrument classes are large enough to hold an entire bottle.

Figure 2: Bottle in the measurement position in front of an integrating sphere in the MPC-2600. The measuring window is 1 x 2.5 cm. The bottle can be positioned using the x-y-z table. The measuring window can be seen through this thin transparent bottle.

Measurement results using UV-VIS spectroscopy

There are different approaches for qualification in glass analysis. It is possible to perform a standardized

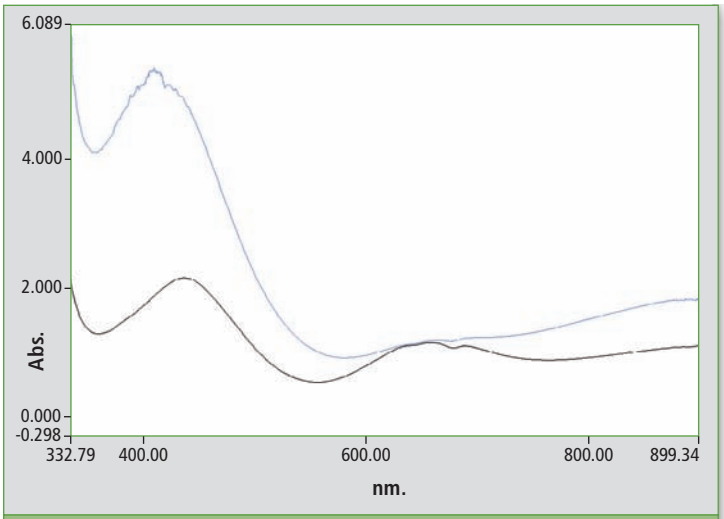

Figure 3: Absorption spectra of glass bottles in the visible spectral range of 310 to 890 nm

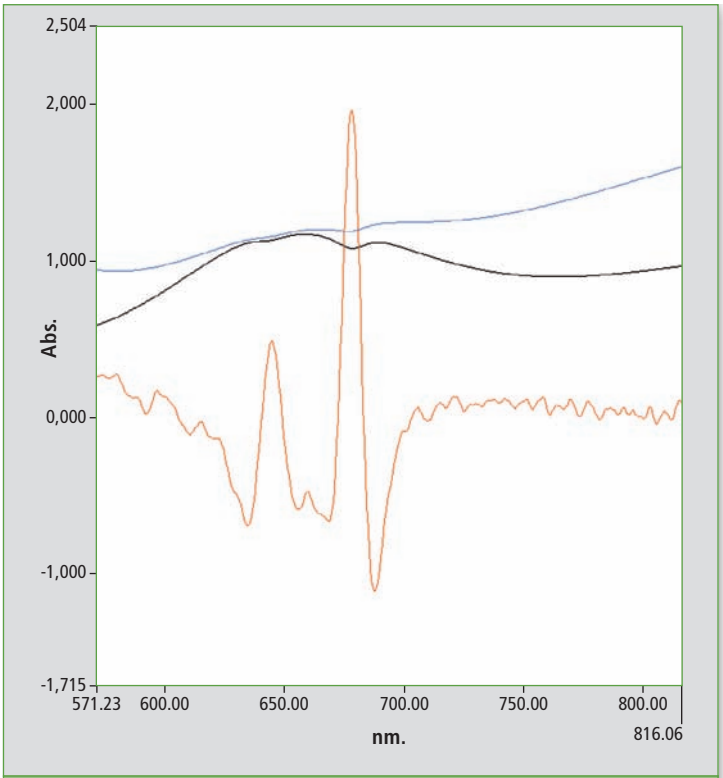

Figure 4: Using the second derivative of the spectrum of the old wine bottle, the energy bands belonging to Cr_2O_3 can be made visible according to the literature [2]

color analysis for which specialized evaluation software is available, for instance Chroma (ILIS) or Color Lite (LabCognition). These color analysis software packages calculate standard color values from the given UV spectrum. These are objective color analysis methods.

Classical evaluation is performed on the spectrum itself. The nature of the oxides and their specific energy potentials yield characteristic UV-VIS spectra. These spectra work like fingerprints, even at high concentrations. Interpretation of the spectra enables classification of the elements that are involved in the coloration of the glass.

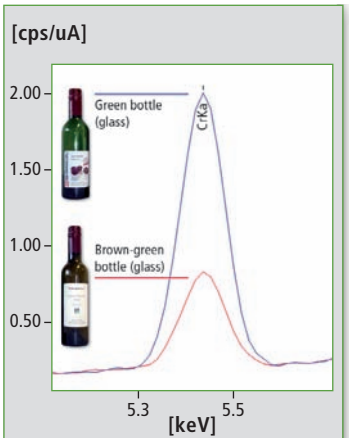

Figure 5: EDX measurement curves of a wine bottle, where blue represents the old wine bottle and red the new wine bottle. The green color of the old bottle is related to its higher Cr content.

Another challenge is the shape of the material, for instance a bottle with thick walls. In the transmission and absorption method, two walls were illuminated. This inevitably leads to strong absorptions. In this analysis, another interfering material is present: the glass itself. It exhibits strong absorptions in the ultraviolet range, which affects the analysis of iron oxides. UV spectroscopic analysis focuses on the color of the solid. In this analysis, the sample material was not destroyed (Figure 2).

In addition to coloring materials, glass also contains other main materials that are required for the properties of the target application. In order to identify these elements, the non-destructive EDX measuring technique is recommended.

Figure 3 shows the absorption spectra of two wine bottles. The black line (bottom) represents the colors and components of the old bottle and the blue line (upper) those of the new bottle. In the spectra, the Fe_2O_3 range (400 - 450 nm) and the Cr_2O_3 range at 650 nm can be clearly recognized. A quantitative shift can be identified in the spectra. The black spectrum (bottom) shows that there is more Cr_2O_3 present, while in the blue spectrum the iron oxide region around 410 nm absorbs more strongly.

Using the second derivative, the oxide fine structure (Figure 4) can be made visible for these spectra that were measured with a resolution of 5 mm.

The increased iron oxide signals in the blue spectrum are a matter for discussion. In the literature, an increase of the signals by manganese oxide has been described [3]. This effect, and the reduction of the chromium oxide, causes the bottle color to change to brown.

tected, is element specific and can therefore be assigned to each element. Due to the presence of glass (SiO_2), a high percentage is assigned to silicon oxide. Since the starting materials used in glass manufacture are silicon oxide and mixtures of other oxides, a range of elements can be expected. The analysis presented was carried out with the fundamental parameters. The observed surface is 1 cm in diameter. For analysis, the bottle is placed directly into the sample compartment.

Two wine bottles of different years were analyzed. Both bottles are used for bottling red wine. As might have been expected, the EDX result was dominated by the typical glass oxides – i.e. SiO_2, CaO and K_2O, which represent the main components in both bottles. A summary of the results is presented in table 2. The results of individual measurements are shown in figures 6 and 7 (Page 18).

Oxide	Color (varies depending on the oxidation level of the element)
Iron oxide	Green, yellow or brown-black
Copper oxide	Blue, red
Chromium oxide	Green
Cobalt oxide	Blue
Manganese oxide	Used to decolorize the green cast
Rare earths	Various colors

Table 1: Typical oxides for staining of glasses [1]

Element	Old wine bottle	New wine bottle
CaO	23,56 %	21,60 %
K_2O	10,736 ppm	13,010 ppm
Fe_2O_3	7,662 ppm	8,640 ppm
Cr_2O_3	4,932 ppm	1,789 ppm
MnO	732 ppm	810 ppm
SiO_2	73.66 %	75.44 %
Property of the color	Green	Green-brown

Table 2: Comparison of the element distribution in both wine bottles

Measurement results using the EDX technique

Using EDX, all elements involved in the composition of the glass can be identified, For the measurement, the bottle is placed on the measurement window. The high-energy radiation of the EDX penetrates the glass, and the elements react to the X-ray irradiation by emitting fluorescence radiation. This fluorescence radiation is de-

```
Sample  : New Shimadzu Wine
Operator:
Comment :
Group   : easy_10mm_solid_glas
Date    : 2014-08-13 10:36:15

Measurement Condition
-------------------------------------------------------------------------------
Instrument: EDX-7000   Atmosphere: Air   Collimator: 10(mm)
-------------------------------------------------------------------------------
Analyte              TG kV   uA      FI   Acq.(keV) Anal.(keV)  Time(sec)    DT(%)
-------------------------------------------------------------------------------
Al-U                 Rh 50   40-Auto ---- 0 - 40   0.00-40.00  Real- 100    29
Na-Sc                Rh 15  342-Auto ---- 0 - 20   0.00- 4.40  Live-  30    29

Quantitative Result
-------------------------------------------------------------------------------
Analyte               Result           [3-sigma] Proc.-Calc. Line   Int.(cps/uA)
-------------------------------------------------------------------------------
CaO                216023.2 ppm        [820.157] Quan-FP    CaKa      60.1445
K2O                13010.04 ppm        [177.567] Quan-FP    K Ka       2.9257
Fe2O3               8640.910 ppm        [73.025] Quan-FP    FeKa      40.6842
Cr2O3               1789.420 ppm        [63.732] Quan-FP    CrKa       4.3924
BaO                 1580.463 ppm       [233.593] Quan-FP    BaLa       0.7990
TiO2                1347.062 ppm       [114.795] Quan-FP    TiKa       1.3861
MnO                  810.726 ppm        [41.019] Quan-FP    MnKa       3.0715
ZrO2                 507.743 ppm        [11.705] Quan-FP    ZrKa      14.3686
SO3                  433.802 ppm       [358.370] Quan-FP    S Ka       0.0219
PbO                  350.857 ppm        [24.869] Quan-FP    PbLb1      3.3818
SrO                  331.637 ppm        [ 9.694] Quan-FP    SrKa       9.8975
CuO                  282.707 ppm        [18.632] Quan-FP    CuKa       2.8501
Ag2O                 223.758 ppm        [30.476] Quan-FP    AgKa       2.0709
ZnO                  131.424 ppm        [14.720] Quan-FP    ZnKa       1.5868
SiO2                  75.447 %          [ 0.927] Quan-FP    SiKa      21.1973
```

Figure 6: Analysis of the new wine bottle (EDX measurement)

```
Sample  : Old Shim Wine
Operator:
Comment :
Group   : easy_10mm_solid_glas
Date    : 2014-08-13 10:31:44

Measurement Condition
-------------------------------------------------------------------------------
Instrument: EDX-7000   Atmosphere: Air   Collimator: 10(mm)
-------------------------------------------------------------------------------
Analyte              TG kV   uA      FI   Acq.(keV) Anal.(keV)  Time(sec)    DT(%)
-------------------------------------------------------------------------------
Al-U                 Rh 50   40-Auto ---- 0 - 40   0.00-40.00  Real- 100    30
Na-Sc                Rh 15  310-Auto ---- 0 - 20   0.00- 4.40  Live-  30    29

Quantitative Result
-------------------------------------------------------------------------------
Analyte               Result           [3-sigma] Proc.-Calc. Line   Int.(cps/uA)
-------------------------------------------------------------------------------
CaO                235621.2 ppm        [863.851] Quan-FP    CaKa      71.3630
K2O                10736.95 ppm        [157.385] Quan-FP    K Ka       2.6355
Fe2O3               7662.724 ppm        [66.980] Quan-FP    FeKa      37.8581
Cr2O3               4932.159 ppm        [70.385] Quan-FP    CrKa      12.7734
TiO2                 965.559 ppm        [99.887] Quan-FP    TiKa       1.0483
BaO                  941.295 ppm       [203.421] Quan-FP    BaLa       0.5019
MnO                  732.888 ppm        [41.495] Quan-FP    MnKa       2.9334
PbO                  450.079 ppm        [25.686] Quan-FP    PbLb1      4.5544
ZrO2                 433.835 ppm        [10.944] Quan-FP    ZrKa      12.8783
SrO                  279.375 ppm        [ 9.093] Quan-FP    SrKa       8.7470
CuO                  246.846 ppm        [16.969] Quan-FP    CuKa       2.6182
SO3                  174.241 ppm       [335.493] Quan-FP    S Ka       0.0096
ZnO                  133.346 ppm        [14.139] Quan-FP    ZnKa       1.6932
SiO2                  73.663 %          [ 0.883] Quan-FP    SiKa      22.3179
Rb2O                  56.802 ppm        [ 7.770] Quan-FP    RbKa       1.7750
```

Figure 7: Analysis of the old wine bottle (EDX measurement)

Discussion

Using the EDX results, the visual and spectroscopic analyses could be confirmed. It was found that molecular spectroscopy exhibits characteristic signals that could be assigned to the oxides involved. The color as well as the composition could therefore be determined from one spectrum. The EDX elemental analysis complemented the obtained result with additional details of the material, which could indicate that the unexpected element contributions (such as silver) originated from recycled glass.

Literature

[1] Werner Vogel: Glaschemie. 3. Auflage, Springer-Verlag, 1992.

[2] The effect of chromium oxide on optical spectroscopy of sodium silicate glasses, Bahman, Mirhadi, Behzad Mehdikhani, Journal of Optoelectronics and Advanced Materials, Vol. 13, No. 9, September 2011, p. 1067 - 1070

[3] Effect on manganese oxide on redox iron in sodium silicate glasses, Bahman, Mirhadi, Behzad Mehdikhani, Journal of Optoelectronics and Advanced Materials, Vol. 13, No. 10, October 2011, p. 1309 - 1312

Coffee inspired not only science

Particle measurement using the SALD-2300

»Design while drinking wine, execute while drinking coffee.« With these words, Jean Paul, a writer in the Romantic period, bestowed literary honors on coffee and associated the stimulating effects of coffee with creative work. But coffee not only helps writers at their desks, but also helps scientists to endure long nights at the laboratory – and who knows to which fundamental

SALD-2300

achievements coffee was the steaming witness. But have any researchers in this situation ever wondered about the history and origin of this exotic beverage?

According to legend, a shepherd noticed his animals behaving oddly: they were still fit and awake, and were hopping around in spite of the approach of night. He found out that his lively sheep had nibbled on the red berries of a kaffa bush, which apparently caused this odd behavior.

And whether he ate the berries and noticed the same effects himself or whether he brought the berries to monks who experimented with the beans and created brews – here the stories start to diverge.

One thing is certain, however: the coffee bush and the coffee bean (which in botanical terms is the pit of a fruit resembling cherries) originate from the province of Kaffa in the forested highlands of southeast Ethiopia. Several centuries would pass, however, until coffee conquered the entire world.

Enjoyment depends on many factors

Coffee is a science in itself. Not only is the entire process of planting, harvesting, cleaning, and preparing the coffee challenging and requiring a professional eye, but downstream processes such as roasting are also important.

Of course, brewing a good cup of coffee also has to be learned. The appropriate temperature, the correct mixing ratio of water and ground coffee, the water pressure and many other influences such as grind settings of the coffee beans will add a particular flavor.

The degree of grinding of the coffee beans determines the taste of the coffee. Using the SALD-2300 particle size analyzer (measuring range 17 nm - 2,500 µm, concentration range: 0.1 ppm - 20 %) with the DS-5 dry measurement unit, various coffees were measured. For a single measurement, a volume of approximately 0.5 - 1 cm^3 was needed. In addition to the type of coffee and degree of roasting, the fineness of the grind was a crucial difference.

It has become apparent that the oil and overall moisture content of powdered coffee pose a particular challenge for measurement. Individual particles can stick together easily to form larger aggregates. This effect was even slightly exacerbated by vacuum packaging the coffee samples.

After drying the powdered coffee and due to the very efficient double-dispersion process of the dry measurement unit, highly reproducible measurement of the individual samples became possible.

Results

Figure 1 shows measured results of a total of four coffee samples (2 x filter coffee, espresso and mocha). The particle size distribution based on volume ranges from 50 µm, with the first maximum at approximately 150 µm, via a second maximum at approximately 700 µm, to a particle size of approximately 1,500 µm.

The SALD-2300 with its numerous accessories is suitable for virtually any application. In addition to dry particle measurement, the SALD-2300 can be used for wet-dispersion particle measurement. Accessories such as the BC-23 and the MS-23 are available for this purpose. Even highly concentrated pastes with a particle concentration of up to 20 % can be measured using the optional HC-23 accessory.

Coffee – four popular brewing methods

Depending on tradition, culture and personal taste, there are hundreds of ways coffee can be brewed. However, almost all brewing methods fall into one of the following basic preparation methods. The coffee is ground to a different degree for each of these methods.

Filter coffee
This brewing method is especially popular in the U.S. and in Germany. In the method developed in 1908 by Melitta Bentz from Dresden, Germany, medium-finely ground coffee is placed in a paper filter bag and extracted by pouring hot water over it.

French press
As the name says, this brewing method is especially popular in France. The coarsely powdered ground coffee is placed directly in hot water and is subsequently separated from the water using a press plunger and metal sieve before pouring the coffee into cups.

Espresso method
In this method, water is forced through finely ground coffee under a pressure of 9 - 15 bar. As a result, a layer of foam generally known as 'crema' is formed from the coffee's oils. The espresso method is very popular in Italy and other countries.

Turkish coffee or mocha
This brewing method (and actually also the type of coffee itself) was named after the port city of Al Mukah on the Red Sea. Here, an ultra-finely ground coffee (resembling powdered sugar) is mixed with the same amount of sugar, and this mixture is boiled for several minutes in a copper kettle. The mocha is ready for drinking when the coffee grounds have settled at the bottom of the cup.

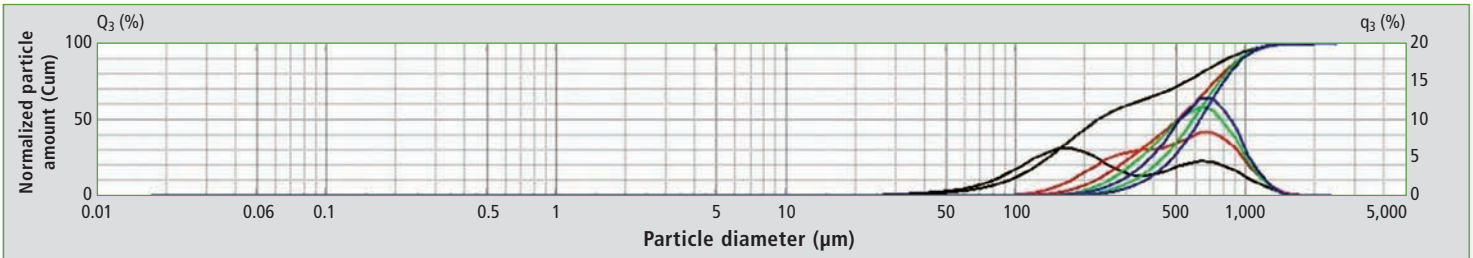

		File name	Absorbance	Ref. index	Median diameter	Modal diameter	Mean value	Standard deviation	1,000.0 µm	800.0 µm	500.0 µm	315.0 µm	125.0 µm
1	—	Coffee_001	0.000	3.00-0.20i	226.457	161.963	256.396	0.372	95.401	89.149	71.955	60.421	20.651
2	—	Coffee_002	0.000	3.00-0.20i	500.501	675.330	472.267	0.243	93.019	81.169	49.693	25.447	0.824
3	—	Coffee_003	0.000	3.00-0.20i	587.659	675.330	566.298	0.181	93.236	78.979	35.491	9.179	0.042
4	—	Coffee_004	0.000	3.00-0.20i	630.067	675.330	606.458	0.169	92.228	75.257	28.157	5.956	0.026

Figure 1: Particle size distribution of four different coffee samples

Hidden danger

LCMS-8050 – Faster and more sensitive detection of mycotoxins in baby food

They are natural and part of the biosphere, but they are toxic for humans and animals – mycotoxins are metabolic products of lower fungi, which also include molds. They are formed during improper storage of food or feed materials, or under adverse conditions such as increased humidity or elevated temperatures before harvest in the field. Since acute poisoning rarely occurs, these substances attract little attention.

Although very high levels of mycotoxins can act acutely toxic, the highest hazard potential, however, lurks in their carcinogenicity, mutagenicity and teratogenicity when taking up low quantities over an extended period of time. Furthermore, it has to be assumed that the accumulation of mycotoxins in the human body is responsible for the development of organ diseases such as nerve, kidney, liver and heart damages.

Contamination with fungi or their mycotoxins in the field or during storage is a serious problem, also for agriculture worldwide. According to estimation of the Food and Agriculture organizations of the United Nations (FAO) up to 25 % of the world production of grains and derived staple foods are infested with mycotoxin producing fungi. Mainly grains, oily seeds and nuts, coffee, fruits, vegetables as well as spices are affected.

Nexera X2 combined with Triple Quadrupole mass spectrometer LCMS-8050

Introduction of limits

Since 2006, uniform maximum levels in certain foods have been applied in Europe for the protection of consumers. These maximum levels are dependent on the toxicity of the mycotoxin as well as on the intended use of the food. Processing into baby food is particularly critical, as these little consumers have special needs. The body of a small child is particularly sensitive to toxic compounds, because of their low body weight, their higher metabolic rate and their poorly developed ability to detoxify contaminants and foreign substances (xenobiotics). The European Commission has, therefore, specified very low limits, especially for infant and child nutrition.

The lowest levels apply to the highly toxic ochratoxin A (0.025 µg/kg), as well as to aflatoxins B1 (0.1 µg/kg) and M1 (0.025 µg/kg) because they belong to the most potent carcinogens.

A sensitive analysis for the protection of very young consumers is therefore essential. This application presents a new method for ultra-fast analysis of mycotoxins in various types of baby food using the LCMS-8050 triple-quadrupole mass spectrometer. The following foods were examined in detail: powder for the preparation of baby milk, milk thickening cereals, flour, rice and tapioca, as well as a vegetable purées mixed with cereals.

Materials and methods

Sample preparation:
20 mL of a water-acetonitrile mixture (volume ratio 1 : 1) was added to the homogenized sample (5 g), treated for 5 minutes in an ultrasonic bath and subsequently agitated for additional 30 minutes at room temperature. After centrifugation (3,000 g, 10 min.), the supernatant was diluted with water (volume ratio 1 : 4). The extraction columns (Isolute® Myco, Biotage, Sweden; 60 mg / 3 mL) were first conditioned with 2 mL acetonitrile and then with 2 mL water. 3 mL of the diluted supernatant were transferred onto the extraction column at the lowest possible flow rate.

This was followed by two washing steps, first with 3 mL of water,

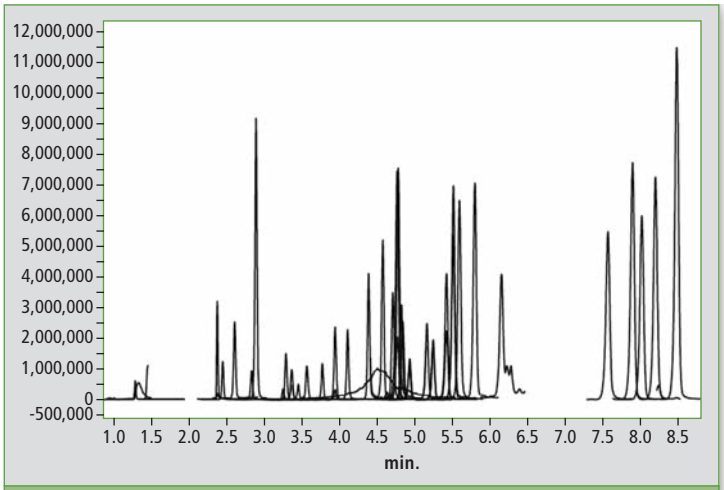

Figure 1: Chromatogram of a mycotoxin standard with 45 components at a concentration of 50 ppb (2 ppb for the aflatoxins and ochratoxins)

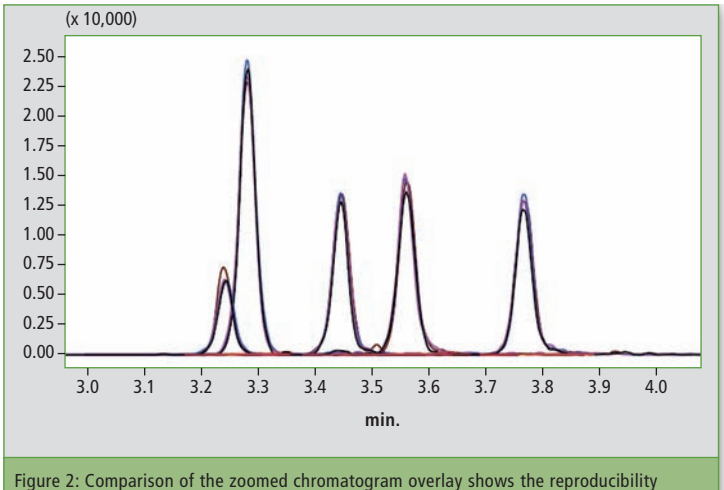

Figure 2: Comparison of the zoomed chromatogram overlay shows the reproducibility (n = 4) for 5 aflatoxins (c = 0.1 ppb) in grain flour, which is added to infant milk as a thickening agent

History and discovery of mycotoxins

Older than mankind and widespread all over the world, toxins of molds have attracted the interest of researchers not till recent decades. Already in the Bible, there are reports on a disease that occurs after ingesting ergot. And in the Middle Ages, hundreds and thousands fell victim to this disease that is known today as ergotism (St. Anthony's fire). Even mysterious phenomena in history, such as the decline of many advanced civilizations or mystic deaths of about 30 persons that were involved in the opening and exploration of the tomb of the Egyptian pharaoh Tutankhamun, can most likely be traced back to acute mycotoxin poisoning.

Also in recent times, there have been repeated reports on initially mysterious diseases that were later associated with the deadly effect of molds. For instance, at the beginning of the 20th century, a disease caused by the fusarium fungus (in moldy sorghum and wheat) was mentioned in the former Soviet Union, that probably first appeared in the year 1891 and took hundreds and thousands human lives until the end of World War II (source: Determination of aflatoxins and patulin using online SPE-LC by Andreas Sascha Wendt).

The first mycotoxins were discovered and identified not until in 1961 the cause of the mysterious death of 100,000 turkey poults was investigated in England. After an intensive search, the researchers encountered aftlatoxins in the moldy animal feed. During the following years, there was a virtual explosion of discoveries of new toxic metabolites of molds. That these compounds could also be present in human nutrition and be the cause of diseases only became evident over time, when optimized analytical methods and modern instrument technology became available that enabled sensitive and fast monitoring of foods and food ingredients.

So far, approximately 300 different mycotoxins are known that are produced by more than 250 molds during their growth (source: German Federal Institute for Risk Assessment – BfR, Bundesinstitut für Risikobewertung). Of these, only some are relevant for food and feed safety. These include:

- **Aflatoxins**
- **Ochratoxins**
- **Ergot alkaloids**
- **Fusarium mycotoxins (trichothecenes, fumonisins, zearalenone)**
- **Patulin.**

Mycotoxins are not visible and may remain in foods, even after removal of the fungi. Highly processed foods, in which detection of any fungi is often very difficult or no longer possible, may still contain mycotoxins. Conversely, foods that on visual inspection are clearly infested with fungi do not necessarily contain mycotoxins, although consumption is strongly discouraged.

As mycotoxins are chemically very stable compounds and thermally stable up to very high temperatures, they are generally not destroyed during food processing. A so-called 'carry-over' effect is found in farm animals that have consumed toxin-containing feeds. Certain mycotoxins can be deposited in unchanged or metabolized form in various organs or can be excreted.

This way, mycotoxins get into foods of animal origin (meats, eggs, milk, milk products) without the product being moldy itself. Also this type of contamination is not externally recognizable. Using sensitive analytical instrumentation, however, detection and identification is possible even at extremely low concentrations.

followed by 3 mL water-acetonitrile (volume ratio 9 : 1). After drying, the components were eluted stepwise from the column, starting with 2 mL acetonitrile, acidified with 0.1 % formic acid, followed by 2 mL methanol. The eluate was evaporated to complete dryness at 35 °C under nitrogen (Turbovap, Biotage, Sweden). The sample was mixed with 150 µL of a solvent mixture (water/methanol/acetonitrile at a volume ratio of 80 : 10 : 10 and 0.1 % formic acid).

LC-MS/MS analysis:

The extract was analyzed using a *Nexera* X2 UHPLC system (Shimadzu, Japan) coupled to Shimadzu's LCMS-8050 triple-quadrupole mass spectrometer. Sample analysis was carried out in the MRM mode (Multiple Reaction Monitoring) with two transitions per component. The parameters of the ion source and the interface, i.e. gas flows, voltages and temperatures, were carefully optimized, so that due to their synergistic effect, the optimal sensitivity could be achieved with the LCMS-8050. Parameter optimization is important especially for the critical analytes, in this case the aflatoxins.

45 mycotoxins in less than nine minutes

Figure 1 shows the chromatogram of a mycotoxin standard with a concentration of 2 ppb for the aflatoxins (B1, B2, G1, G2, M1) and ochratoxin A and B, as well as 50 ppb for the remaining mycotoxins.

As criterion for the quality of the analysis method, the recovery rates of the sample preparation (extraction recovery) were determined, as well as the matrix effect during ionization (ionization recovery) for the aflatoxins. The measurements were carried out in 3 different matrices. Table 1 lists the values for vegetable-grain purée (comparison of the peak areas of matrix spiked with standards before or after extraction, as well as the comparison with the peak areas of a pure standard solution).

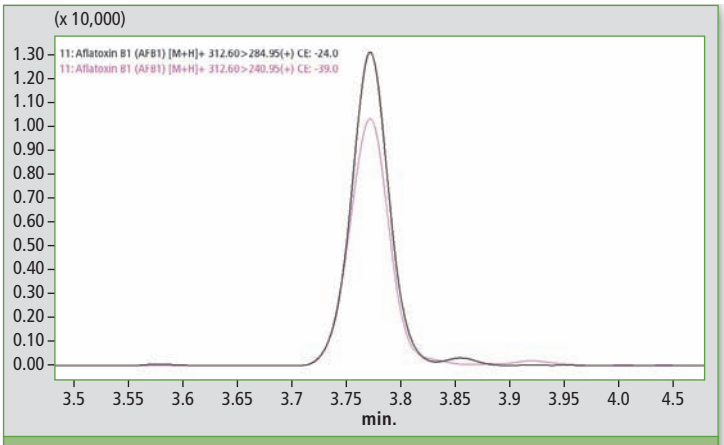

Figure 3: Aflatoxin B1 at a concentration of 0.2 ppb

	AFB1	AFB2	AFG1	AFG2	AFM1
Extraction recovery	101 %	109 %	104 %	114 %	118 %
Ionisation recovery	49 %	90 %	96 %	106 %	91 %
Total recovery	49 %	98 %	100 %	121 %	108 %

Table 1: Recovery rates of the aflatoxins in vegetable-grain purée

The results for the recovery rates in the two other matrices (baby milk powder, milk thickening cereals) do not differ much from the values listed in table 1. In addition, the reproducibility of the analysis results was investigated. Figure 2 shows the good reproducibility (n = 4) of the aflatoxins at a concentration of 0.1 ppb in the matrix (matrix in this example: milk thickening cereals).

Figures 3 and 4 clearly show that the required legal limit value of 0.1 µg/mL for aflatoxin B1 (MRM Quan 312.6 > 284.9, MRM Qual 312.6 > 240.9) as well as 0.025 µg/mL for aflatoxin M1 (MRM Quan 329.1 > 237, MRM Qual 329.1 > 229) is easily attained.

Conclusion

Because of its high toxic and carcinogenic potential, reliable and sensitive determination of mycotoxins is essential, especially for the protection of infants and young children.

The present application describes a reliable method for the quantification of 45 mycotoxins in baby food. With the ultrafast scan rates of the LCMS-8050 and a polarity change of only 5 ms, the analysis takes less than nine minutes. Recovery rates and reproducibility measurements in three different baby foods illustrate the reliability of the method.

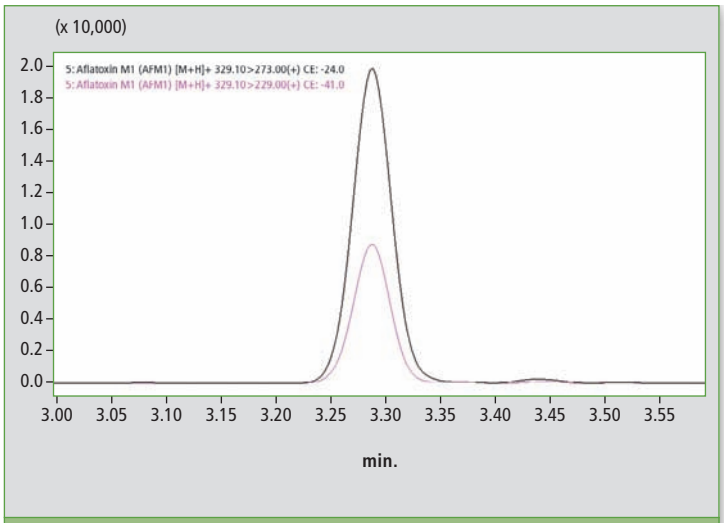

Figure 4: Aflatoxin M1 at a concentration of 0.2 ppb

Biomass fuel: can algae make the wheels go round?

Monitoring of algae growth by TOC measurement

Global warming due to excessive use of fossil fuels has prompted and accelerated the search for alternative fuels. Among the more interesting alternatives is biomass fuel, which has attracted considerable attention.

Microalgae can be used for the production of oil without competing with food production. Compared with other biofuels, its productivity per unit time and area is high, while arable land selection possibilities are immense. As for the practical use of microalgal biomass, various studies have been conducted at each stage of its production, including stock selection and breeding, cultivation, harvesting, oil extraction and purification.

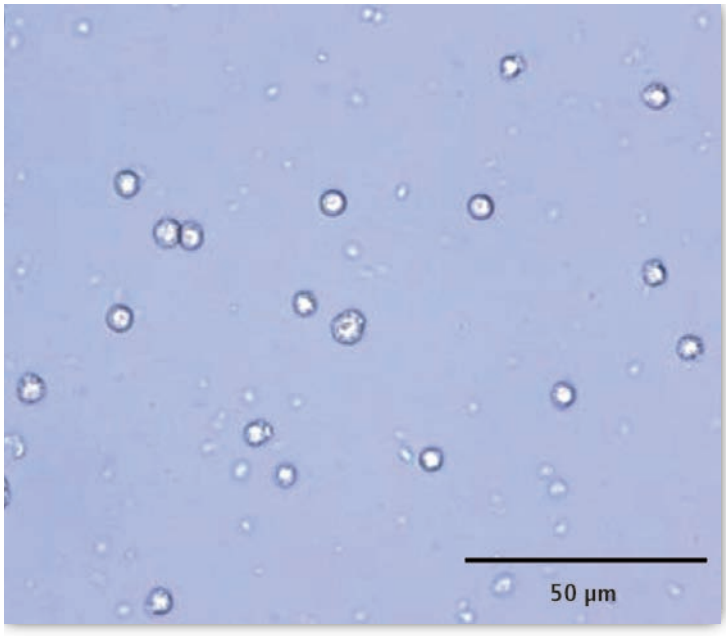

Figure 1: A microscopic image of the microalgae cells of sample 1

The Shimadzu TOC-L series combustion-type total organic carbon (TOC) analyzer with its powerful organic substance oxidation features enables complete oxidization and measurement of samples such as microalgae cell culture suspensions.

In this unique application the TOC-L is used to track the growth process of microalgae by measuring the TOC content directly in a suspended culture of microalgae cells. No pretreatment is necessary.

The data presented are provided by Prof. Yoshihiro Shiraiwa's laboratory at the University of Tsukuba, Japan.

Analytical method

The microalgae was cultured for eight days. As of the first day, TOC measurement was conducted once per day for both sample 1 (consisting of a culture along with suspended microalgae cells) and sample 2 (with a culture only obtained by removing the microalgae cells from sample 1 through centrifugal sedimentation). Based on the difference in organic carbon (TOC) between sample 1 and sample 2, the value of TOC present for the organic matter of the microalgae cells was then obtained. Further, the turbidity of sample 1 was measured and the

value used as an index of cell mass. A microscopic image of the microalgae cells of sample 1 is shown in figure 1.

Measurement Conditions

- Analyzer: Shimadzu TOC-L$_{CPH}$ total organic carbon analyzer
- Catalyst: Standard catalyst
- Measurement item: TOC (TC-IC)
- Calibration curve: 1-point calibration curve using 1,000 mg/L potassium hydrogen phthalate aqueous solution
- Sample 1: Culture solution containing suspended microalgae cells
- Sample 2: Culture solution with microalgae cells removed using centrifugal sedimentation Water sampling method: Sample 1 water was sampled while stirring with a magnetic stirrer.

Measurement results

Figure 2 shows the measurement results for the total carbon (TC), total organic carbon (TOC) and inorganic carbon (IC) associated with the cell mass during the culture period. The ratios of TOC to IC in the microalgae cells are also shown in figure 3. From these results, it was possible to obtain information on increase and decrease of TC, IC and TOC values associated with the microalgae cells throughout the culture process.

One essential element in the practical realization of microalgal biomass is to establish the culture conditions, and this study demonstrates that information regarding the carbon balance can be obtained using a TOC analyzer.

Shimadzu TOC-L series total organic carbon analyzer

The TOC-L can be used to conduct the following types of measurements:

- Total carbon and nitrogen content in water, quantity dissolved, quantity suspended
- Total carbon, organic carbon, inorganic carbon in water
- Dissolved CO_2 in water

The TOC-L can therefore be used in applications of microalgae research such as:

- Obtaining information on the physiological state and properties of microalgae
- Understanding changes in cell material in the culture over time and due to light and dark environment
- Understanding quantitatively the carbon and nitrogen balance in the culture system.

The TOC-L can be used to conduct measurements using very small sample volumes in the range of 10 to 20 mL, making it suitable for laboratory-scale studies.

Abbildung 4: TOC-L-Gesamtkohlenstoffanalysator plus TNM-L-Gesamtstickstoffeinheit

The TNM-L total nitrogen unit option is required for nitrogen (TN) measurement. In addition, filtering and centrifugal separation etc. are required for separate measurement of samples in the dissolved and suspended state.

IMPRINT

Shimadzu NEWS, Customer Magazine of Shimadzu Europa GmbH, Duisburg

Publisher
Shimadzu Europa GmbH
Albert-Hahn-Str. 6-10 · D-47269 Duisburg
Phone: +49-203-7687-0
Fax: +49-203-766625
shimadzu@shimadzu.eu
www.shimadzu.eu

Editorial Team
Uta Steeger
Phone: +49 (0)203 76 87-410
Ralf Weber, Tobias Ohme

Design and Production
m/e brand communication GmbH GWA Düsseldorf

Circulation
German: 5,450 · English: 6,680

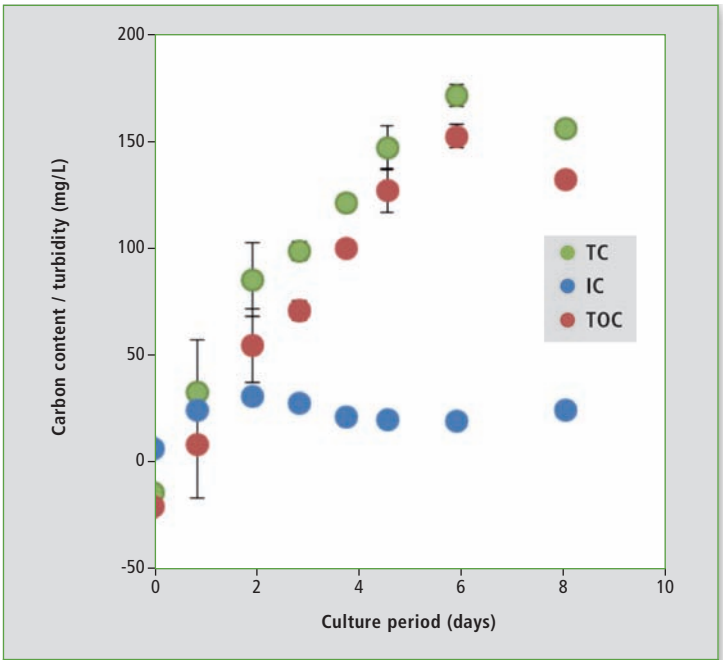

Figure 2: Changes in TC, IC, TOC quantity in microalgae cells (conversion value per turbidity unit)

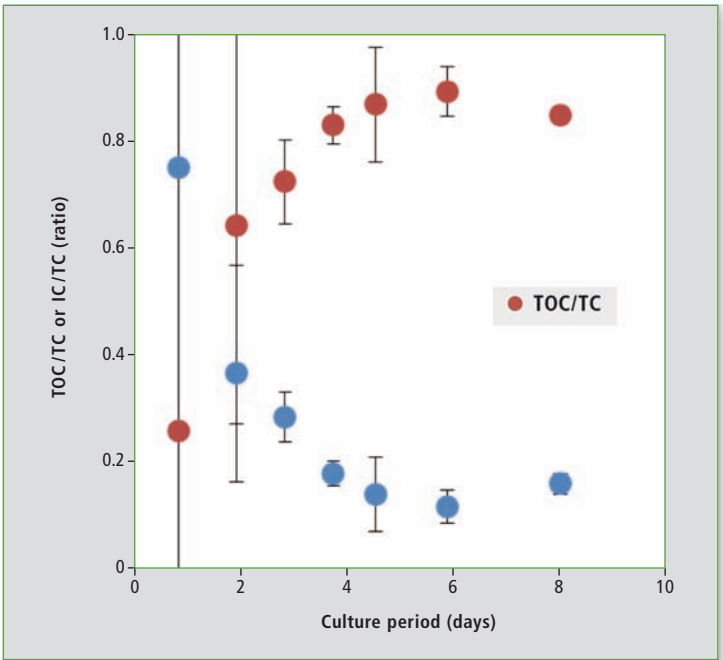

Figure 3: Changes in TOC/TC and IC/TC in microalgae cells

Sweet secrets analyzed fast and easily

Automated validation procedure of an optimized UHPLC assay

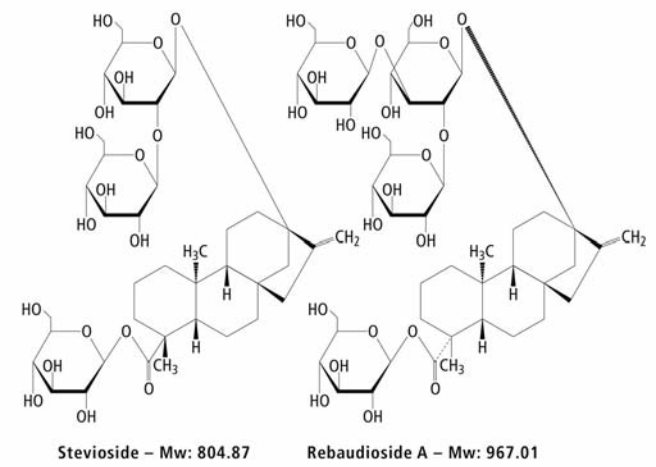

Figure 1: Structures of stevia glycosides

With today's growing health awareness, there is an increasing interest in sugar substitutes in various areas of the food industry. Compared to well established artificial sweeteners, such as Aspartam and Saccharin, the natural alternative Stevia, extracted from the Stevia rebaudiana plant has been approved for use in the EU only in 2011. Stevia, also known as sweet-leaf, is native to South America and the plant extract contains steviol glycosides with up to 450 times the sweetness of sugar.

As the Rebaudioside A steviol glycoside exhibits the lowest bitter aftertaste, it is largely enriched in commercial stevia products, while natural extract contains stevioside as the major component. Hence, an HPLC assay for quality control purposes, must be able to clearly separate this critical peak pair. After method development using the *Nexera* X2 Method Scouting Platform, the *Nexera-i* new generation integrated UHPLC system with its system check function and automated workflow was the ideal tool for a quick and simple programmed method validation procedure.

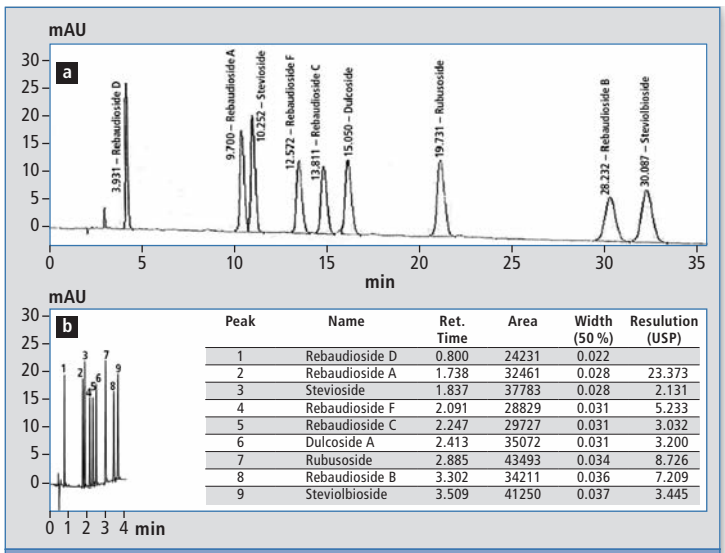

Peak	Name	Ret. Time	Area	Width (50 %)	Resulution (USP)
1	Rebaudioside D	0.800	24231	0.022	
2	Rebaudioside A	1.738	32461	0.028	23.373
3	Stevioside	1.837	37783	0.028	2.131
4	Rebaudioside F	2.091	28829	0.031	5.233
5	Rebaudioside C	2.247	29727	0.031	3.032
6	Dulcoside A	2.413	35072	0.031	3.200
7	Rubusoside	2.885	43493	0.034	8.726
8	Rebaudioside B	3.302	34211	0.036	7.209
9	Steviolbioside	3.509	41250	0.037	3.445

Figure 2: a) JECFA method for the separation of nine stevia glycosides
b) improved UHPLC assay for the separation of nine stevia glycosides

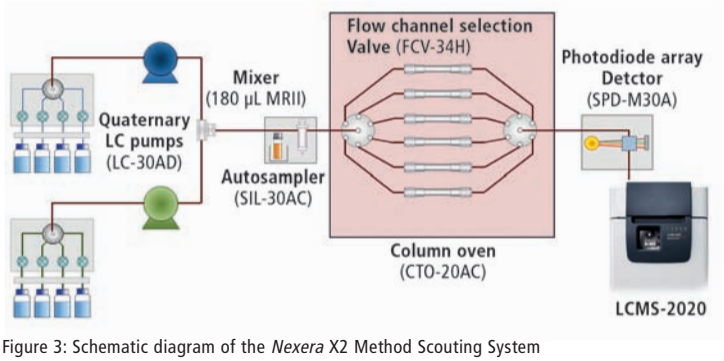

Figure 3: Schematic diagram of the *Nexera* X2 Method Scouting System

Method Development

JECFA method (Figure 2 a):
Column: Phenomenex Luna C18(2) 5 µm; 250 x 4.6 mm
Mobile Phase: A: 10 mM NaH_2PO_4, pH 2.6 in H_2O to B: ACN (68 : 32 v/v)
Isocratic: 35 min run time
Flow rate: 1 mL/min
Temperature: 40 °C
Injection Volume: 5 µL
Sample: 0.2 mg/mL of each compound in MeCN/H_2O (30 : 70 v/v)

For UHPLC method scouting, a Shimadzu *Nexera* X2 Method Scouting System was used, consisiting of two quaternary solvent pumps, an autosampler and a column oven including a six column switching valve. The system was also equipped with a photo diode array detector (Figure 3).

Method scouting was performed in an overnight sequence using 3 and 9 min gradient runs at 30 °C and 50 °C. Five combinations of stationary phase and mobile phase were selected. The data obtained from the most promising mobile phase/stationary phase combination was used for computer simulation to identify the optimum separation conditions with respect to gradient slope and oven temperature.

Resulting UHPLC method (figure 2 b)

Column: ACE Excel 2 Super C18, 150 x 2.1 mm
Mobile Phase: 10 mM NaH_2PO_4, pH 2.8 A: in H_2O and B: in MeCN/H_2O (80 : 20 v/v)
Gradient: 39.5 - 48 % B in 4 min
Cycle time: 7 min
Flow rate: 0.6 mL/min
Temperature: 50 °C
Injection Volume: 1 µL
Sample: 0.04 mg/mL of each compound in MeCN/H_2O (6 : 94)

Validation

The method obtained was fully validated using the LabSolutions / VALIDAT interface. The incorporated template assistant required merely the addition of the appro-

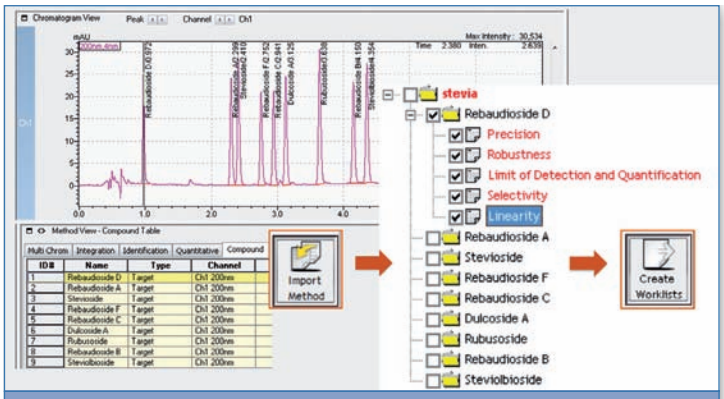

Figure 4: Validation planning by method import from LabSolutions into VALIDAT©

priate components to be validated, which was achieved by importing the LabSolutions method file (.lcm) with compound table into the VALIDAT project (Figure 4).

To carry out the validation successfully, the software provided all mathematical and statistical procedures, as well as full 21 CFR Part 11 compliance. With a well-structured workflow and versatile, adjustable templates the validation process was organized easily and efficiently (Figure 5).

After importing the method, each parameter, such as precision, linearity, repeatability etc. was planned individually. According to these checkpoints VALIDAT released a validation plan as a starting point for programmed batch creation in LabSolutions. By importing the batch from VALIDAT into LabSolutions each data file (.lcd) obtained a unique identifier that allowed automated export of the analytical results back into the validation software, eliminating the need for manual copy-pasting and the risk of human error during this process.

Additionally, the *i*-series 'Auto Validation' function (Figure 6) allows to easily evaluate whether or not the system is working in a stable range. System parameters, such as solvent delivery or wavelength accuracy are controlled by a fixed procedure to guarantee the system performance before carrying out a method validation.

It is also possible to carry out an automated routine inspection and self-diagnosis of the instrument via the 'System Check' function, where data on consumable usage is recorded, such as number of injections, solvent volume delivered by the pump or UV lamp burn time. The results of the auto validation and system check procedures are summarized in a printed report that can be added to the validation documents.

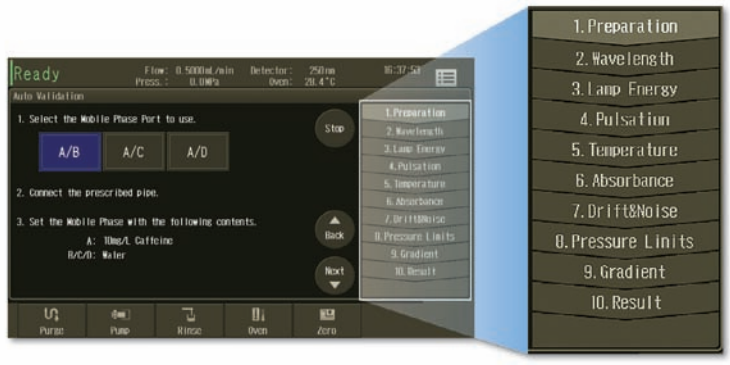

Figure 6: Auto-validation procedure in *i*-series instrument

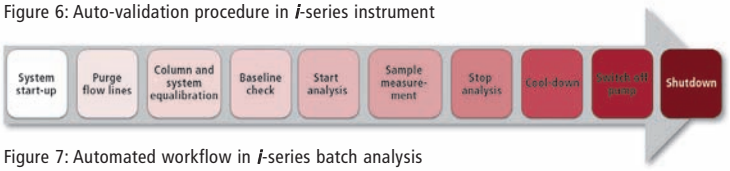

Figure 7: Automated workflow in *i*-series batch analysis

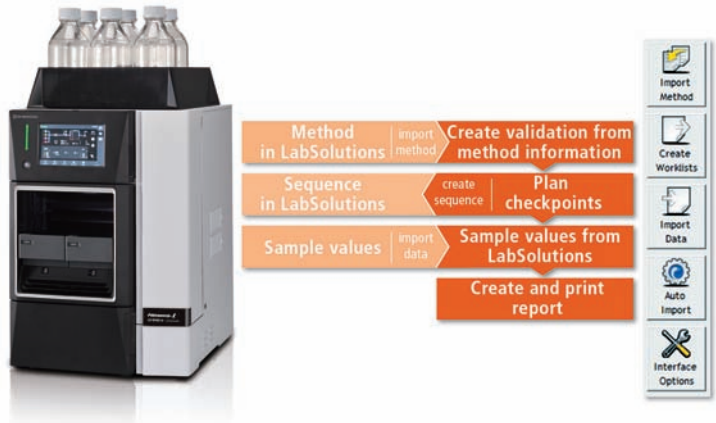

Figure 5: Method validation workflow guided by VALIDAT©

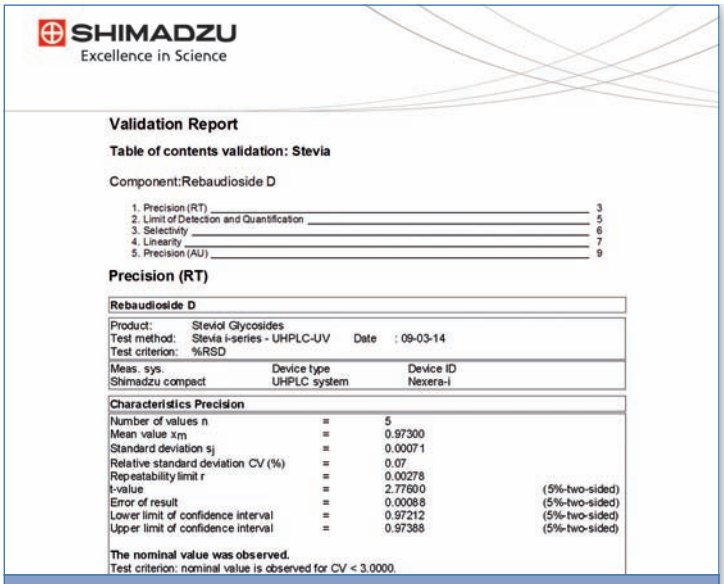
SHIMADZU
Excellence in Science

Validation Report

Table of contents validation: Stevia

Component:Rebaudioside D

1. Precision (RT) 3
2. Limit of Detection and Quantification 5
3. Selectivity 6
4. Linearity 7
5. Precision (AU) 9

Precision (RT)

Rebaudioside D

Product:	Steviol Glycosides		
Test method:	Stevia i-series - UHPLC-UV	Date	: 09-03-14
Test criterion:	%RSD		

Meas. sys.	Device type	Device ID
Shimadzu compact	UHPLC system	Nexera-i

Characteristics Precision

Number of values n	=	5	
Mean value xm	=	0.97300	
Standard deviation sj	=	0.00071	
Relative standard deviation CV (%)	=	0.07	
Repeatability limit r	=	0.00278	
t-value	=	2.77600	(5%-two-sided)
Error of result	=	0.00088	(5%-two-sided)
Lower limit of confidence interval	=	0.97212	(5%-two-sided)
Upper limit of confidence interval	=	0.97388	(5%-two-sided)

The nominal value was observed.
Test criterion: nominal value is observed for CV < 3.0000.

Figure 8: Finished validation report created by VALIDAT© according to company template VA

After the system status had been evaluated, the LabSolutions batch file allowed full automation of the sample analysis from starting of the instrument to the shut-down procedure after the run had finished.

All necessary steps, such as switching on the instrument at a defined time, purging of the flow lines, column/system equilibration until a stable baseline was obtained, sample measurements, system wash and shut-down were programmed into the batch table and carried out automatically in an overnight run (Figure 7).

Results

After electronic release of the validation plan for programmed batch creation in LabSolutions and analysis on the *i*-series using the workflow described in figures 4 - 7, the pre-defined validation report (Figure 8) was completed within minutes thanks to the automated data import into VALIDAT. The successfully completed validation project was then saved as a template that will serve as a starting point for further projects.

More freedom of choice

New features in TOC-Control L software

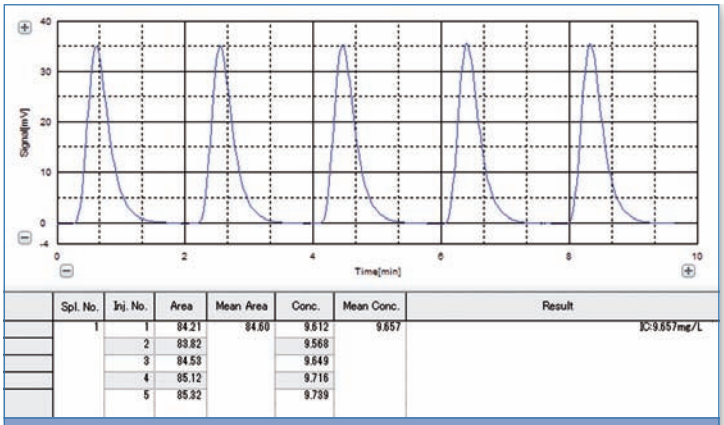

Figure 1: Peak profile of IC measurement for sample A

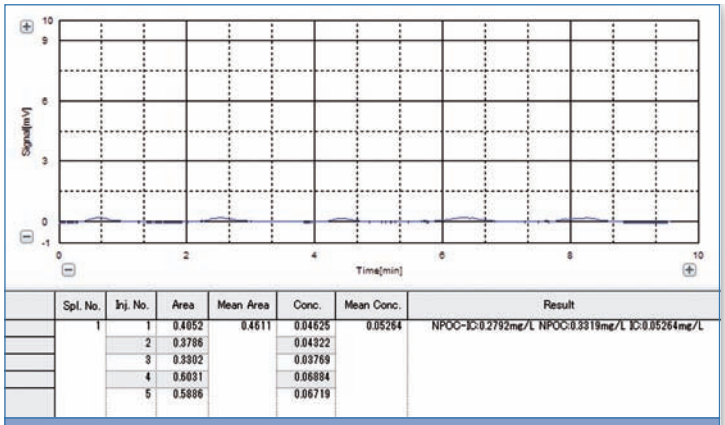

Figure 2: Peak profile NPOC and IC measurement for sample A in case of NPOC-IC type

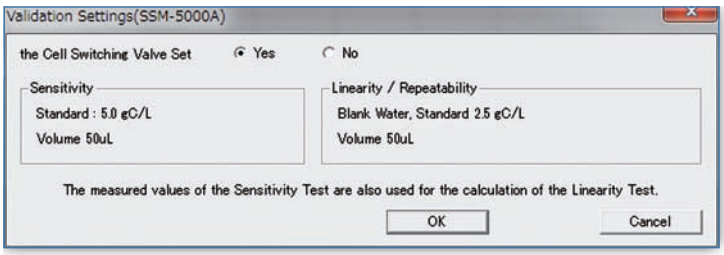

Figure 3: Validation setting dialogue for SSM-5000A

New features and more straightforward operation have been the leading principles in the development of the TOC-Control L software. In combination with this software, Shimadzu's TOC-L series instruments offer users modern tools for straightforward and reliable TOC analysis in all application areas. Shimadzu now releases a new TOC-Control L software providing new valuable features.

Residual inorganic carbon (IC) checks

Key to TOC determination is the difference between organic and inorganic carbon. The most popular method used is the so-called NPOC method in which the sample is acidified to convert the carbonates and hydrogen carbonates, i.e. inorganic carbon (IC) present in the sample to CO_2. The carbon dioxide is subsequently purged using a gas stream passed through the sample.

During NPOC analysis measurement, IC removal may be incomplete depending on pH or other characteristics, and IC may remain inadvertently in some samples. If it's necessary to check the effectiveness of the IC removal treatment, the software will perform IC measurement just after the NPOC measurement and then output results in which the IC values are subtracted from NPOC values.

Automatic re-measurement of samples out of calibration range

With samples of unknown concentration, the TOC-Control L software offers automatic re-measurement when the result exceeds the calibration range. Up to now, the software changed the injection volume and the dilution factor for this purpose. In some applications, it is useful to change the dilution factor only by keeping the same injection volume.

For this case, the new version offers the possibility to select between automatic changing of injection of volume or dilution factor.

Improved support for performing instrument validation

It is necessary to confirm the performance of the instrument at regular intervals in order to guarantee reliability of measurement. For this purpose, TOC-L has a feature to create schedules easily for validation measurements. They can be created quickly and easily using simple window operations and check parameters such as sensitivity, linearity and repeatability.

Furthermore, this feature is also compatible with the SSM-5000A solid sample module for combustion option. The settings dialogue is prepared separately from TOC-L instrument validation settings. From these contents, a sample table for validation can be prepared.

Conclusion

The new TOC-Control L software version gives more freedom to create the optimal method for measuring TOC in specific samples. The improved validation table also reduces validation time.

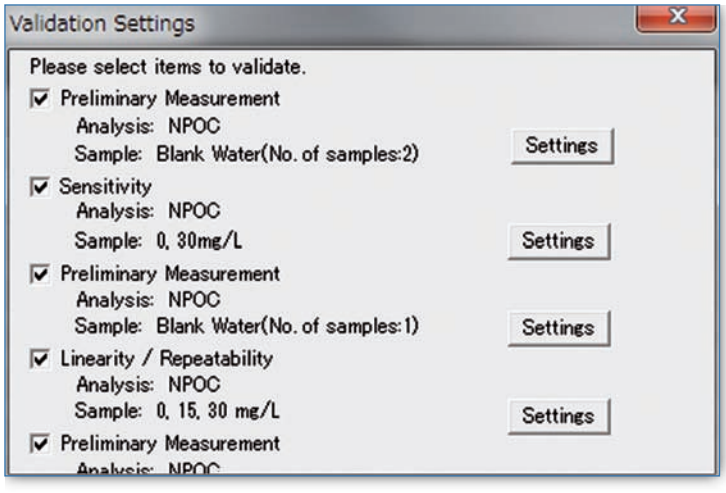

Figure 4: Validation setting dialog for TOC-L

Sparkles in kids' eyes

Shimadzu employees are socially engaged

For Shimadzu and its employees, social and non-profit commitment is day-to-day reality. Fellow citizens as well as the environment take center stage in this corporate-citizen-engagement. Shimadzu has launched various projects in which employees can become socially involved, such as the annual 'Social Day' in Duisburg, or the 'Wish Tree' in which employees fulfill children's Christmas wishes.

In 2013, the first 'Social Day' was organized and tackled enthusiastically by 25 employees. Within the scope of Germany's national 'Maltese Social Day' the Maltese Foundation had recommended to help out in Duisburg's kindergarden 'The little Rascals.' In cooperation with the directors of Shimadzu Europa and Shimadzu Deutschland, Jürgen Kwass and Jürgen Semmler, walls were painted, toys were repaired and garden plots were planted.

Identifying with communities and regions

"As an established Duisburg-based company, Shimadzu is closely connected with the city and the region. The same is true for our technical offices and their respective locations in Germany" explains Jürgen Semmler. "As part of the increased awareness for sustainable development of our society and businesses, Shimadzu has become involved as a responsible company. Therefore, our 'Social Day' is a yearly contribution in which we, together with our employees, commit ourselves to social projects in our region."

After the successful start last year, volunteers were easily found in September 2014 to help out at the Duisburg animal shelter. Various teams undertook various tasks for which there is often no time in daily operation of the shelter. "We renovated and freshly painted the dog pool, built a wooden house, felled a tree and even baked dog biscuits", said Jennifer Libuda. "A little tired, but very proud, at the end of the day we could look back to many accomplished projects."

During advent time – 'Wish Tree' for children

Since 2012, Shimadzu's employees also volunteer with pre-Christmas social events: a 'Wish Tree' realized in cooperation with the Social Welfare Organization Diakoniewerk Duisburg. Children from socially disadvantaged families that are being looked after in day care groups at the Diakoniewerk may write down their Christmas wishes, which are then being fulfilled by Shimadzu employees. In 2012 and 2013, close to 70 children and adolescents received Christmas gifts this way.

During Christmas 2014, Shimadzu was committed again – and because of the current political situation the event took place this time at the refugees' home in Duisburg-Baerl. 63 children could look forward to receiving a Christmas present from Shimadzu employees, who in turn received the greatest gift themselves – sparkles in kids' eyes.

For more about Shimadzu's social commitment see

www.shimadzu.eu/shimadzu-news-2015

Universal testing machine qualifies electronic components

Standardized shear force testing

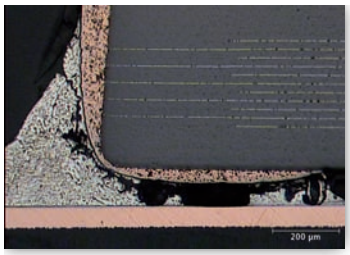

Figure 1: Crack formation at a solder joint due to thermo-mechanical stress (transverse metallographic section)

Modern electronic products must meet a variety of characteristics. They are expected to perform better than their predecessor generations, but they should also be lighter, smaller or more robust. They must be able to withstand environmental influences such as temperature or humidity, and should endure mechanical stresses such as vibration or mechanical shocks – all this combined with an environmentally friendly manufacturing process and lower production costs.

A decisive factor for the reliability of an electronic product is the solder joint [1]. When it fails, the electronic product also fails [2].

Shear force test as classical testing method

Various tests are available to investigate the reliability of solder joints. As a conventional destructive testing method, the shear force test has become well established [3]. Changes in the solder joint that can, for instance, occur due to thermo-mechanical stress can be identified this way. The shear force is the measured quantity, which decreases with increasing degradation of the solder joint [3].

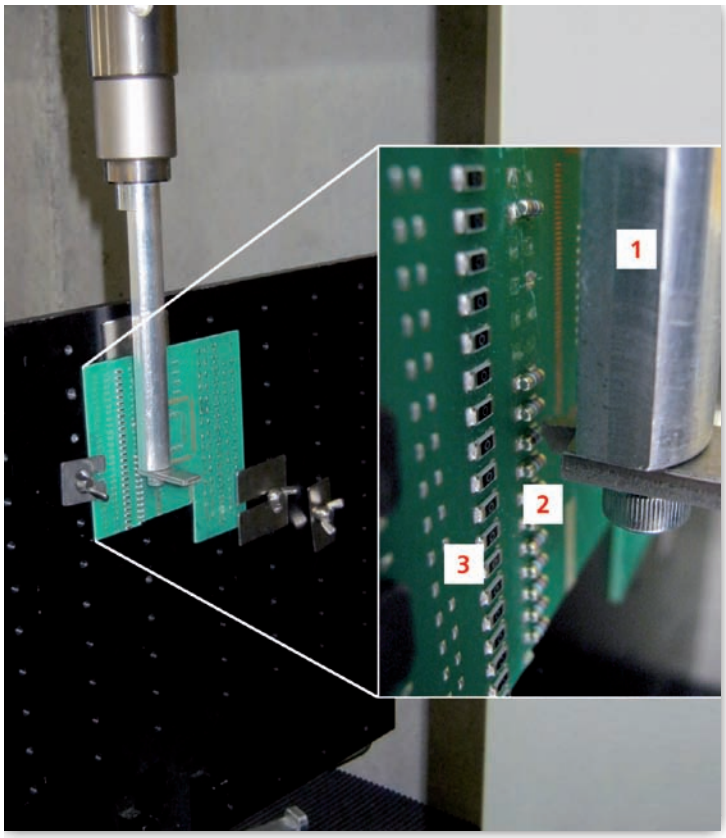

Figure 2: AG-X shear test assembly with (1) = shearing chisel and (2) = M MELF type components (3) = 1206 type components

The tests are normally carried out with a small set of different materials prior to the start of production within the scope of product qualification. As a rule, these include various solder pastes that are necessary for the connection between substrate and component and various printed circuit board metallizations. These tests must also be performed when the solder paste is changed, for instance during an ongoing production process. The shear forces can be determined on real components, for instance on circuit boards of a mobile phone, or on a test assembly. Due to statistical fluctuations of individual component failure it is advantageous to carry out the tests with a sufficient number of identical components [3]. As these are usually not available in large numbers, a test assembly is to be preferred.

The underlying DIN EN 62137-1-2 norm states that the measuring device for carrying out the shear test merely must "include a mechanism for mounting the substrates ..." and "can exert a shear force that is greater than the strength of the soldering connection ..." The recommended feed rates in DIN EN 62137-1-2 are between 0.5 mm/min and 9 mm/min.

Universal testing machine for shear tests

In addition to the specialized shear test devices available on the market it is, consequently, also possible to use a universal testing machine for carrying out shear tests. The Japanese norm JIS Z 3198-7 (2003) [5] explicitly allows the use of a universal testing machine. The speed range for testing specified in the Japanese JIS Z 3198-7 is between 5 mm/min and 30 mm/min. The implementation of the normative standards for carrying out shear tests using Shimadzu's AG-X universal testing machine with the 90° shear test kit is described below.

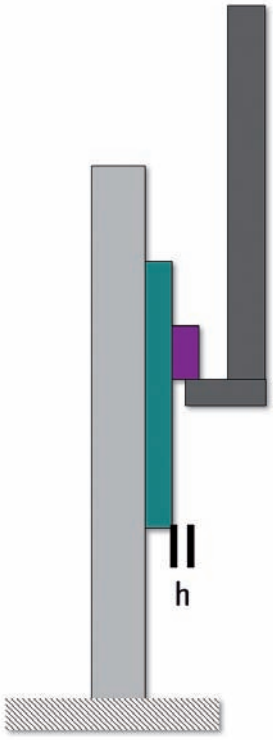

Figure 3: Schematic of the shear test geometry.

A test board with M-MELF and 1206 type components were used as test objects applying a lead-free tin-silver-copper soldering paste and a chemical-gold circuit board metallization, as well as a test circuit board with SMD capacitors in sizes 2512, and also a chemical-gold circuit board metallization using a tin-silver-copper soldering alloy. The individual component types were each soldered in a row onto the circuit board. This leads

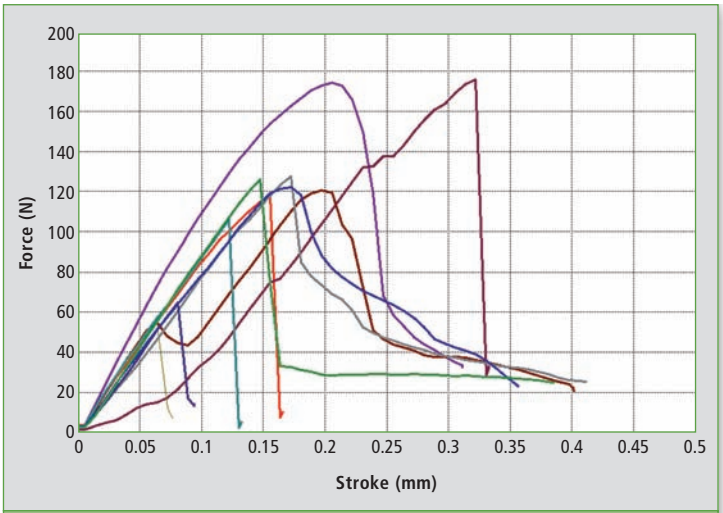

Figure 4: Example of a shear force diagram for ten components of size 2512

to more economical testing procedures, as the circuit board does not need to be readjusted prior to each measurement.

Implementing the shear tests

The circuit board is mounted on the breadboard of the shear test kit with slotted clamping plates and positioned via micrometer screws (Figure 2). It has been proven advantageous to drive the shearing chisel up to the point where it contacts the circuit board. This point can be easily recognized on the micrometer screws, as these will no longer indicate any distinct change in length.

Subsequently, the shearing chisel is adjusted to the desired component distance h via the micrometer screws (see figure 3). A value of 0.1 mm has been found suitable. According to DIN 62137 the shearing height, which is the distance of the circuit board to the shearing chisel, should not be greater than ¼ of the component height. During the shear test, one has to make sure that the shearing chisel does not rub against the solder pad of the circuit board or against the solder deposit.

A stainless steel chisel was custom-made for each component width, which can be screwed onto the standard mount of the shear test kit of the tensile strength testing machine, was used as shearing chisel. The shear rate was set to 5 mm/min and automatic recognition of the sample fracture was activated in the measuring method.

After the start of the measurement and the automatic sample fracture recognition, the sheared component is removed from the shearing chisel using tweezers. The shearing chisel is subsequently moved up to the next component via manual control of the tensile strength testing machine and a further measurement is started.

For evaluation, the maximum strength is primarily of interest. In case of questionable fracture patterns during optical inspection, the force-displacement diagram is used to detect possible non-uniform shearing. This can occur when the shearing chisel has not sheared off the component horizontally, but due to displacement of the component only one side of the component has initially been sheared off. Such shear patterns can be clearly recognized in the force-displacement diagram. Via the overlay function of the Trapezium-X software, it is possible to display several measuring curves superimposed in one diagram (Figure 4). This way, it is possible to evaluate the quality of several solder joints at a glance.

After shearing, the remaining residual solder joints are examined under a microscope and classified according to their fracture mode (Figure 5). In the current example fractures only occurred along the solder/component interface and diagonally across the solder (see figure 5, component a and component b).

Conclusion

After carrying out several hundred shear tests according to the method described, it can be concluded that shear tests can be performed according to the relevant standards using a universal testing machine. A comparison of the determined shear forces with the shear forces documented in the literature [6] shows a similar dispersion of the measurement results.

To determine the influence of soldering defects, such as porosities on the shear forces and their dispersion, it is possible to first examine the samples using a non-destructive method, for instance 2D X-ray testing or computer-assisted tomography and to classify them according to their proportion of porosities [7].

Due to the typical features of the universal testing machine, it is also possible to carry out cyclic tests on SMD components without shearing, using custom-made shearing chisels. The first of such tests carried out have been promising so far.

Acknowledgement

Achaffenburg University of Applied Sciences thanks Shimadzu for its professional support and collaboration as well as for supporting our teaching and research activities.

Author

Prof. Dr. Michael Kaloudis
Aschaffenburg University of Applied Sciences, laboratories for materials technology and structural-design and connection technologies

References

[1] Shnawah DA, Sabri MFM, Badruddin IA (2012) A review on thermal cycling and drop impact reliability of SAC solder joint in portable electronic products. Microelectronics Reliability. Doi:10.1016/j.microrel.2011.07.093

[2] Suganuma K (2001) Advances in lead-free electronics soldering. Current Opinion in Solid State and Materials Science. Doi:10.1016/S1359-0286(00)00036-X

[3] Dusek M (2002) Test methods for evaluating the reliability of PCB finishes using lead-free alloys: A guide. MATC A 107. National Physical Laboratory, Teddington

[4] DIN Deutsches Institut für Normung e.V. Oberflächenmontage-Technik – Verfahren zur Überprüfung von Umwelteinflüssen und zur Prüfung der Haltbarkeit von Oberflächen-Lötverbindungen Teil 1-2: Scherfestigkeitsprüfungen. Beuth Verlag (DIN EN 62137-2)

[5] Test methods for lead-free solders. JIS Z 3198-1 2003. Japanese Standards Association, Tokyo, Japan

[6] Ahrens T, Andreae H, Schruttke W (2006) RoHS-Handbuch für Hersteller und Zulieferer: Praktische Umsetzungshilfen, alternative Materialien und innovative Verfahren. Forum Verlag Herkert, Merching

[7] Rauer M, Volkert A, Schreck T, Härter S, Kaloudis M (2014) Computed Tomography-Based Analysis of Voids in SnBi57Ag1 Solder Joints and Their Influence on the Reliability. J Fail. Anal. and Preven. Doi:10.1007/s11668-014-9801-y

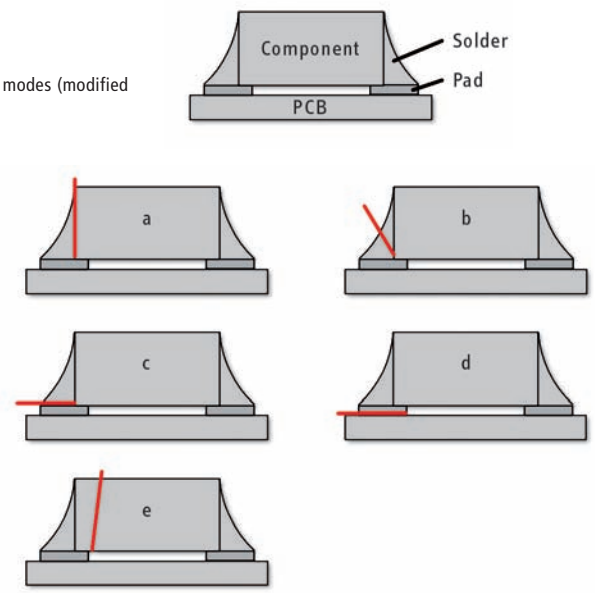

Figure 5: Fracture modes (modified according to [6])

High sensitivity meets robustness

Gas measurements – Unique BID plasma technology for ppb detection limits

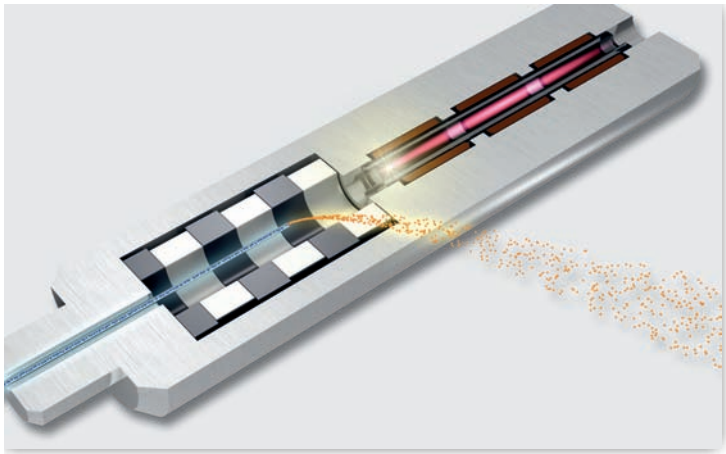

Figure 1: Cross-sectional drawing of a BID detector. Introduction of the discharge gas and helium plasma generation takes place in the upper half of the detector, while detection of the components eluting from the capillary column takes place in the lower half.

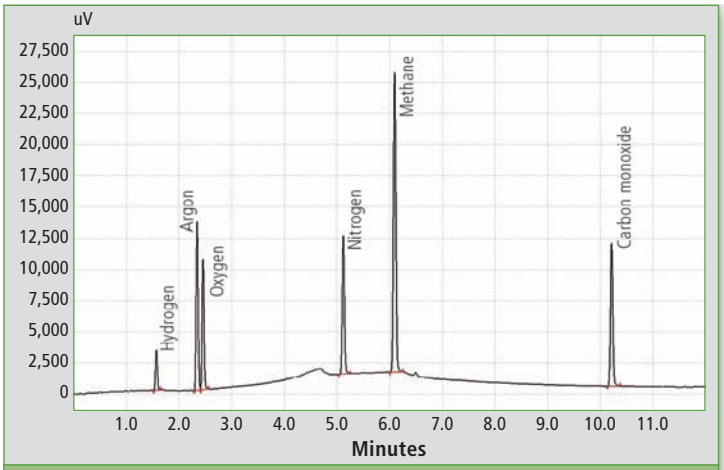

Figure 2: Standard chromatogram of permanent gases and hydrocarbons

Gas chromatography is a common technique in monitoring of complex gas samples emitting from exhaust, process supervision or quality control of gases. Detection limits in the ppb range are often required so that without extensive enrichment technique, injection of a sample volume of 500 - 1,000 µL requires a very sensitive detection system. Furthermore, gas samples normally consist of several components (e.g. permanent gases and hydrocarbons), so a universal detection system is needed.

The Flame Ionization Detector (FID) is popular due to its exceptional combination of sensitivity, reproducibility and long-term stability. Unfortunately, the FID detection spectrum lacks permanent gases such as oxygen, nitrogen and carbon dioxide. On the other hand, while Thermal Conductivity Detectors (TCD) are universal detectors, they operate in the ppm detection range and are therefore not sensitive enough.

In gas chromatography, helium ionization technique has become an interesting solution that allows universal detection of all components with high sensitivity. Detection limits in low ppb range are achievable without any extensive sample enrichment techniques. However, easy operation and long-term stability of systems operated in trace analysis is still challenging.

Unique plasma technology

Shimadzu's new Barrier Ionization Discharge Detector (BID) combines high sensitivity of helium ionization technique with robustness and excellent long-term stability. The unique technology generating the helium plasma allows detection of components with an ionization potential below 17.6 eV. In this way, the detector can see all components except helium and neon.

The helium plasma generation is done within a thin quartz glass tube, building a dielectric barrier between the electrodes and the plasma (Figure 1). In this way the plasma generating electrodes are shielded from contamination by the sample and effects from the plasma itself – one reason for the superior long-term stability of the BID detector. The light emitted from the helium plasma leads to ionization of components eluting from the chromatographic column. Ions generated in this way are detected by special 'kovar alloy' collection electrodes which are another special development contributing to the stability of BID.

Excellent trace capabilities

The quality control of high purity helium is a good example showing the trace capabilities of the BID detector. The chromatogram in figure 2 shows the result of a standard containing hydrogen, argon, oxygen, nitrogen, methane and carbon monoxide in concentrations from 3 to 5 ppm. The gas was sampled and injected by a 6 port 1/16" valco valve with sample loop of 500 µL and equipped with helium purged rotor housing. The gas sample was split 1:1 and injected on a Restek Molsieve column RT-Msieve 5A 30 m ID 0.53 mm df 50 µm. Starting with the temperature program at 0 °C, baseline separation of argon and oxygen was achieved with a chromatographic resolution of R > 1.65.

Detection and quantification limits for the components are shown in table 1 and are calculated on a signal to noise ratio S/N = 3.3 for the detection limits, and on S/N = 10 for the quantification limits. The reproducibility of the respective components over 5 measurements ranged from RSD = 1.1 - 1.5 %.

For baseline separation of argon and oxygen the temperature pro-

Peak#	Retention time	Name	Area	Height	S/N	Detection limit	Quantitative limit	Unit
1	1.571	Hydrogen	8099	3227	63	259	784	ppb
2	2.343	Argon	34905	13433	263	48	146	ppb
3	2.455	Oxygen	27565	10449	205	48	147	ppb
4	5.12	Nitrogen	31747	11032	216	66	199	ppb
5	6.094	Methane	77124	23986	470	25	77	ppb
6	10.214	Carbon monoxide	35627	11464	225	55	165	ppb

Table 1: Detection limits calculated on a signal to noise ratio S/N = 3.3 and quantification limits calculated on S/N = 10

gram was started below room temperature, so active cryogenic cooling of the oven with liquid nitrogen or carbon dioxide is required. Since the BID has almost equal response factors (peak area/concentration) for argon and oxygen, this can be avoided if a sum concentration for both components would be sufficient. The BID response for argon 9.11 area cts/ppb is very similar to oxygen 9.19 area cts/ppb, so the concentration error evaluating both components as sum peak would therefore be less than 1 %.

Figure 3 shows a chromatogram of an unknown helium sample with purity 6.0. The absence of nitrogen and oxygen in the chromatogram proves that the leak rate of the system against ambient air was below the respective detection limits of 48 and 66 ppb respectively. A small concentration of just 68 ppb methane was measured in the high purity helium.

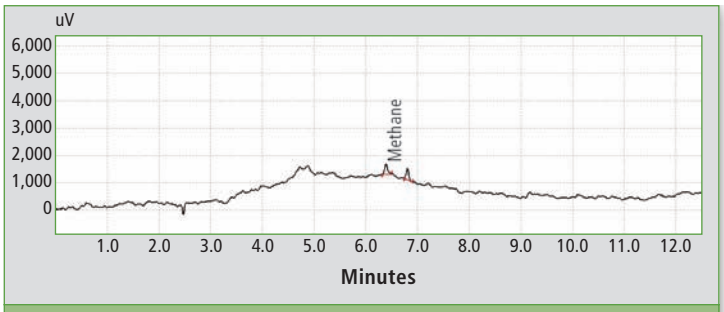

Figure 3: Sample from helium gas cylinder with purity 6.0

Suitable for many applications

High sensitivity and robustness make the Barrier Ionization Discharge Detector (BID) an interesting solution for many applications which would require two or more detectors in order to achieve detection limits in the ppb range. Based on its sensitivity, it can replace a FID detector for analysis of hydrocarbons, thereby improving detection limits by a factor of two or more in the case of small alcohols, aldehydes or acids for which FID is less sensitive. For permanent gases, the BID achieves 200 times better detection limits compared with TCD detector, allowing trace analysis in low ppb range. Because of its robustness and long-term stability the BID is the ideal solution for replacement of TCD and FID combination, which is often used for measurements of gaseous samples containing permanent gases and hydrocarbons.

Performance meets design

Gold Award for the new EDX-7000/EDX-8000 spectrometer series

The EDX series provides outstanding performance: Faster, improved sensitivity, better resolution and no need of liquid nitrogen - these are only a few new features of Shimadzu's next generation of energy dispersive X-ray fluorescence spectrometer targeting material and elemental analysis.

The new EDX-7000 and EDX-8000 inherit the superior features of the successful and established instruments EDX-720 and EDX-800 and provide outstanding additional functions, such as

- an energy resolution better than 140 eV, reducing significantly the impact of coexisting elements
- improved sensitivity which makes LLD's much better
- higher speed providing the same quality of results in 1/10 of the measurement time
- Due to the increased performance and quality of SDD detectors in the recent past, Shimadzu implemented high performance SDD detectors in its new instrument series allowing liquid nitrogen free analysis.

EDX-7000/EDX-8000

The measurement range starts from carbon in case of the EDX-8000, respectively sodium in case of the EDX-7000. Both instruments determine element concentrations up to Uranium. Collimators, camera and filter are standard accessories. Turret, vacuum and helium unit are optional accessories.

Like in the predecessor software, the users have full access to all functions of the software. They can even create calibration curves on their own, no further costs arise.

The instrument is delivered with two software packages: An easy software pack for regularly recurring tasks, and an advanced software pack for professional use.

Industrial Design Gold Award

The new EDX-7000/8000 energy-dispersive (ED) XRF spectrometer has achieved the Gold Award in the Analytical Instrument Industrial Design segment of the 2014 IBO Industrial Design Awards.

It was donated for the system's round front and streamlined profile that sets it apart from other benchtop ED-XRF systems, making the EDX-7000/8000 series approachable and distinctive.

Extended analysis possibilities

Special accessories for the UV-3600 Plus

With the new UV-3600 Plus, Shimadzu has extended its successful UV-VIS-NIR family. The innovation of working with three detectors (PMT [photomultiplier] InGaAs [indium-gallium-arsenide] and PbS cell [lead sulfide]) in the previous UV-3600 model is being continued with additional new accessories.

The MPC-603 (Multi Purpose Sample Compartment) with built-in integrating sphere and ISR-603 (Integrating Sphere Attachment) complement the UV-3600 Plus market introduction. In addition to conventional measurements of diffuse and specular reflectance, it is now also possible to carry out absolute reflectance measurements with three detectors in the UV-3600 Plus.

The sample compartment of the UV-3600 Plus is designed in such a way that on the one hand the PMT is switched off when the sample compartment is open, while also being able to implement accessories connections in the sample compartment. The new integrating spheres are equipped with suitable accessories, allowing measurement of liquids and solids as well as measurement of films.

The most important new features at a glance:

- **ISR-603**
  Cell, powder and film holders are standard equipment for the 60 mm ISR-603 $BaSO_4$ (barium sulfate) integrating sphere. The sphere is equipped with three detectors. The ISR-603 measures diffuse reflectance and total reflectance of liquids and solids. Incidence angles of 0 °C and 8 °C can be realized.

- **MPC-603**
  The sample compartment for large samples is equipped with a 60 mm $BaSO_4$ integrating sphere. Transmittance as well as reflectance measurements can be carried out. Radiation incidence angles of 0 °C and 8 °C onto the sample can be realized. The sample table can be freely adjusted in the xyz direction. It is equipped with a V-stage for non-planar samples that is suitable, for instance, for bottles or large objectives. The MPC-603 can be extended to achieve absolute reflectance measurements for incidence angles of 5°, 12°, 30° and 45°. It contains three detectors for measuring the UV-VIS-NIR radiation.

UV-3600 Plus

UVProbe 2.50 with connection to the LabSolutions platform

The new UVProbe 2.50 software version can be integrated in the database, and can also be integrated as a client-server version in the LabSolutions server platform. This way, the application range is extended from simple file management using Windows Explorer into two additional digital data management versions. The LabSolutions platform works with databases of different levels and integrates a wide selection of instruments, for example chromatography or spectroscopy systems.

Using the LabSolutions connection kit for the UVProbe software, the file version of the UVProbe is converted into a database control component that meets all demands associated with a protected database, such as user level or testing criteria, which are required by pharmaceutical industry regulatory procedures.

Shimadzu live

Laborama	Anakon	Wasser Berlin International	Setac	Control
March 19 - 20, 2015 Brussels, Belgium www.expo.laborama.be	March 23 - 27, 2015 Graz, Austria www.analytchem.tugraz.at/anakon2015/	March 24 - 27, 2015 Berlin, Germany www.wasser-berlin.de	May 3 - 7, 2015 Barcelona, Spain www.setac.org	May 5 - 9, 2015 Stuttgart, Germany www.control-messe.de

If you would like to receive the Shimadzu News on a regular basis, please email us your postal address via: shimadzu-news@shimadzu.eu

You can also subscribe to our newsletter via: www.shimadzu.eu/newsletter

Registration Newsletter

YouTube
@ShimadzuEurope